



North Atlantic right whale density surface model for the US Atlantic evaluated with passive acoustic monitoring

Jason J. Roberts^{1,*}, Tina M. Yack¹, Ei Fujioka¹, Patrick N. Halpin¹, Mark F. Baumgartner², Oliver Boisseau³, Samuel Chavez-Rosales⁴, Timothy V. N. Cole⁵, Mark P. Cotter⁶, Genevieve E. Davis⁵, Robert A. DiGiovanni Jr.⁷, Laura C. Ganley⁸, Lance P. Garrison⁹, Caroline P. Good¹⁰, Timothy A. Gowan¹¹, Katharine A. Jackson¹¹, Robert D. Kenney¹², Christin B. Khan⁵, Amy R. Knowlton⁸, Scott D. Kraus⁸, Gwen G. Lockhart¹³, Kate S. Lomac-MacNair¹⁴, Charles A. Mayo¹⁵, Brigid E. McKenna⁴, William A. McLellan¹⁶, Douglas P. Nowacek^{17,18}, Orfhlaith O'Brien⁸, D. Ann Pabst¹⁶, Debra L. Palka⁵, Eric M. Patterson¹⁰, Daniel E. Pendleton⁴, Ester Quintana-Rizzo¹⁹, Nicholas R. Record²⁰, Jessica V. Redfern⁸, Meghan E. Rickard²¹, Melanie White²², Amy D. Whitt²³, Ann M. Zoidis¹⁴

¹Marine Geospatial Ecology Laboratory, Duke University, Durham, NC 27708, USA

Full author addresses are given in the Appendix

ABSTRACT: The Critically Endangered North Atlantic right whale *Eubalaena glacialis* entered a population decline around 2011. To save this species without closing the ocean to human activities requires detailed information about its intra-annual density patterns that can be used to assess and mitigate human-caused risks. Using 2.9 million km of visual line-transect survey effort from the US Atlantic and Canadian Maritimes conducted in 2003–2020 by 11 institutions, we modeled the absolute density (ind. km⁻²) of the species using spatial, temporal, and environmental covariates at a monthly time step. We accounted for detectability differences between survey platforms, teams, and conditions, and corrected all data for perception and availability biases, accounting for platform differences, whale dive behavior, group composition, and group size. We produced maps of predicted density and evaluated our results using independently collected passive acoustic monitoring (PAM) data. Densities correlated positively ($r = 0.46$, $\rho = 0.58$, $\tau = 0.46$) with acoustic detection rates obtained at 492 stationary PAM recorders deployed across the study area (mean recorder duration = 138 d). This is the first study to quantify the concurrence of visual and acoustic observations of the species in US waters. We summarized predictions into mean monthly density and uncertainty maps for the 2003–2009 and 2010–2020 eras, based on the significant changes in the species' spatial distribution that began around 2010. The results quantify the striking distribution shifts and provide effort- and bias-corrected density surfaces to inform risk assessments, estimations of take, and marine spatial planning.

KEY WORDS: *Eubalaena glacialis* · Density models · Line-transect surveys · Passive acoustic monitoring · Abundance estimation · Generalized additive models

*Corresponding author: jason.roberts@duke.edu

1. INTRODUCTION

The recovery of the Critically Endangered North Atlantic right whale *Eubalaena glacialis* (hereafter 'right whale') is at a tipping point. After falling from a pre-whaling estimated abundance of 9000–21 000 to fewer than 100 in 1935 at the end of commercial whaling, the population increased to a post-whaling peak of 481 in 2011 before declining again to only 340 in 2021 (Monsarrat et al. 2016, Pace et al. 2017, Pettis et al. 2023). For 2003–2018, 88% of necropsied whales died from human-caused injuries (fishing gear entanglements and vessel strikes) (Sharp et al. 2019). When calves are excluded, the causes of death for necropsied adults and juveniles for which cause of death could be determined were all human-related.

Historically, right whales exhibited an annual migration cycle in which a portion of the population moved around the feeding grounds of the Gulf of Maine (GOM) and southwestern Nova Scotia (Canada) in a general counterclockwise pattern (Kenney et al. 2001, Brillant et al. 2015), while some animals migrated in the winter to calving grounds along the continental shelf of the southeastern USA, mainly off Florida and Georgia (Gowan et al. 2019). Starting around 2010, this pattern changed as climate change-driven oceanographic shifts drove declines in prey availability (primarily copepods) at the traditional summer feeding grounds, and a large portion of the population was subsequently documented in the Gulf of St. Lawrence (GSL), exposing it to new gear-entanglement and vessel-strike risks (Davies & Brillant 2019, Record et al. 2019, Simard et al. 2019, Crowe et al. 2021, Meyer-Gutbrod et al. 2021, 2023). The usage of Cape Cod Bay (CCB) in the winter and spring increased substantially (Ganley et al. 2019, Pendleton et al. 2022), and migration to the calving grounds decreased (Gowan et al. 2019). Right whales began inhabiting southern New England (SNE) waters in increasing numbers, primarily in winter and spring (Leiter et al. 2017), but eventually sightings in this area were documented year-round (Quintana-Rizzo et al. 2021, O'Brien et al. 2022). Despite the rise in numbers in SNE and the GSL, a nontrivial fraction of the population remains unaccounted for in summer, likely foraging in unknown locations that lack protection measures (Crowe et al. 2021). The combination of reduced prey availability and frequent injury has not only increased the mortality rate but has also led to reduced calving frequency, body condition, body length, and many other aspects of population health (Moore et al. 2021, Stewart et al. 2021, 2022, Knowlton et al. 2022, Reed et al. 2022).

To arrest the decline of right whales, managers require a detailed understanding of the intra-annual distribution of the species, so that risks can be assessed and mitigated. Research groups have conducted visual surveys for right whales and other protected species since the late 1970s (Cetacean and Turtle Assessment Program 1982). In the 1990s, advances in electronic tagging technology allowed a limited number of individual whales to be tracked by satellite telemetry (Mate et al. 1997). In the early 2000s, researchers began deploying stationary passive acoustic monitoring (PAM) instruments to detect right whale vocalizations (Gillespie 2004, Mellinger 2004). Despite these advances, it remains infeasible to continuously monitor more than a small fraction of the population by any of these modes of observation, and implantable tagging may be detrimental to whale health (Davies & Brillant 2019). As an alternative, researchers can build models of the species' distribution by linking available whale observations to environmental covariates such as seafloor depth and sea surface temperature (SST) (Moses & Finn 1997, Good 2008, Keller et al. 2012, Pendleton et al. 2012, Gowan & Ortega-Ortiz 2014, Wikgren et al. 2014, Monsarrat et al. 2015, Roberts et al. 2016, Gowan et al. 2021, Ross et al. 2021). These models can then be applied to time series of covariate maps collected by satellite remote sensing or extracted from ocean models, to hindcast or forecast corresponding maps of the species' distribution, filling in spatial and temporal gaps in survey coverage.

In the USA, the Marine Mammal Protection Act (16 USC §§ 1361–1423) generally prohibits intentional 'takes' (harm or disturbance) of marine mammals and stipulates the rules under which takes are allowed to occur incidentally during human activities. Within the National Oceanographic and Atmospheric Administration (NOAA), the National Marine Fisheries Service (NMFS, or NOAA Fisheries) regulates the incidental take of marine mammals under its jurisdiction that may result from such activities, and is required to estimate the number of incidental takes that would occur and implement monitoring and mitigation measures to minimize them. In the case of takes resulting in mortality and serious injury (M/SI) incidental to commercial fisheries, if the number of actual takes exceeds a statutory threshold known as the Potential Biological Removal (PBR) level, NMFS must take steps to further evaluate and reduce M/SI takes. For right whales, the number of known human-caused M/SI incidental to commercial fishing has exceeded PBR in nearly all years since 1993 (Kenney 2018).

The need to estimate and reduce marine mammal takes in commercial fisheries, as well as from other human sources, has prompted the development of models that estimate the count or probability of harmful interactions. Harmful interactions are often estimated using the spatiotemporal co-occurrence of the species and activity of interest (e.g. Martin et al. 2016, Crum et al. 2019, Derville et al. 2023). This requires estimates of the number of individual animals and the amount of harmful activity likely to be present at the location. Density surface modeling (Hedley & Buckland 2004, Miller et al. 2013) is a widely used method for estimating animal density (ind. km⁻²) from line-transect or point-transect surveys and has been applied to cetaceans throughout the world (e.g. Williams et al. 2011, Hammond et al. 2013, Roberts et al. 2016, Chavez-Rosales et al. 2019, Becker et al. 2022). A density surface model (DSM) has 2 stages. In the first stage, known as the detection model, distance sampling (Buckland et al. 2001) is used to model the probability of animals being detected given their distance from survey transects and other covariates that affect detectability. The detection model corrects for animals that were present but not detected. In the second stage, known as the spatial model, the corrected abundance on transect segments is modeled from spatial, temporal, or environmental covariates, traditionally using a generalized additive model (GAM; Wood 2017) that relates abundance to covariate values extracted from remote sensing or ocean models.

Here, we present a right whale DSM for US Atlantic waters and a portion of the Canadian Maritimes. The model, initially developed by Roberts et al. (2016) and updated several times, has been used by federal agencies to assess and mitigate risks from activities such as trap and pot fishing (86 FR 51970), vessel traffic (Garrison et al. 2022, 87 FR 46921), naval testing and training (84 FR 70712), and offshore energy activities (<https://www.fisheries.noaa.gov/national/marine-mammal-protection/incidental-take-authorizations-other-energy-activities-renewable>). NOAA Fisheries and the US Navy were the principal funders of the model. As such, they were given the opportunity to suggest goals for each update and recommend spatial and temporal resolutions and a geographic extent that would facilitate the use of the results in US management applications. When the model was complete, they were given the opportunity to review the preliminary results. To maintain the independence of the model, the funders did not participate in the analysis of the data or the preparation of this manuscript beyond the scientific contributions of the individual NOAA coauthors.

The goals of this update, known as version 12, were to redevelop the model using cetacean surveys conducted through 2020; to characterize regional density changes that began around 2010; to estimate density prediction uncertainty with a method that accounts both for uncertainty in model parameter estimates and for temporal variability in model covariates (Miller et al. 2022); and to evaluate density predictions using PAM detections (Davis et al. 2017). (Although DSMs may be used to estimate population abundance, this was not a goal here, as our study area did not encompass the full range of the species. The photographic mark–recapture model of Pace et al. 2017 is better suited to estimating population abundance.) The density predictions may be freely downloaded from the OBIS-SEAMAP model archive (<https://seamap.env.duke.edu/models/Duke/EC/>), and additional technical details about the model are available there as a supplementary report (https://seamap.env.duke.edu/seamap-models-files/Duke/EC/North_Atlantic_right_whale/v12.2/NARW_v12.2_report.pdf) to which we will refer throughout this paper.

2. MATERIALS AND METHODS

This analysis used the same overall methodology as our 2016 model (Roberts et al. 2016) with several improvements and substantial additional data (Roberts et al. 2023).

2.1. Survey data, study area, and time period

We built this model from shipboard and aerial visual line-transect surveys for marine mammals. For a survey to be used in our model, observers must have accurately tracked the position of the survey vessel or aircraft, the times observers went on and off watch, the distances and bearings to sighted animal groups, and the number of animals in each group. Animals must have been detected before they moved in response to the survey platform. Transects must have been laid out in a pre-planned systematic design. Data from surveys conducted haphazardly, or routed directly to known locations of whales, could not be used. NOAA's 2010–2019 Atlantic Marine Assessment Program for Protected Species (AMAPPS; Palka et al. 2021) and its predecessor programs met these requirements and covered the entire study area. However, during 1999–2020, AMAPPS and its predecessors only sighted 120 right whale groups and provided limited coverage in non-summer months. To increase sighting counts and

non-summer coverage, we incorporated surveys from numerous regional programs conducted by 11 collaborating institutions (see Section 3).

Until the 2010s, a substantial fraction of the right whale population migrated between winter calving grounds along coastal Florida and Georgia and summer feeding grounds in the GOM and deep basins of the Canadian Maritimes (Kenney et al. 2001). Consistent surveying of these areas reached an important milestone in 2003 when the right whale Early Warning System (EWS) aerial surveys started monitoring the calving grounds using the same survey protocol across all teams (Gowan & Ortega-Ortiz 2014), and the NMFS Northeast Fisheries Science Center's (NEFSC's) North Atlantic Right Whale Sighting Survey (NARWSS) program started monitoring the GOM with bubble-window Twin Otter aircraft (Cole et al. 2007). Pursuant to our goal of characterizing regional density changes that began in approximately 2010, we built most of our model from surveys conducted during 2003–2020. To increase

sighting counts in August–September in the GOM, when most whales had migrated to Canadian waters, we extended our temporal window back to 1999 to obtain additional NEFSC surveys covering Canada. For surveys monitoring the calving grounds, where extensive effort and sightings were available, we restricted the model to transects with Beaufort sea states of 3 or less (Gowan & Ortega-Ortiz 2014). Elsewhere, where effort and sightings were sparser, we accepted up to Beaufort 4 or 5, depending on the survey program and data availability. In all locations, we excluded transects with poor weather or limited visibility for surveys that reported those conditions, and accounted for the influence of sea state, weather, visibility, and other factors on the probability of making a sighting (see Section 2.2.1).

The full study area extended from the southern tip of Florida (USA) to the Laurentian Channel off eastern Canada, and from shore to the edge of the US exclusive economic zone and the 2000 m isobath in Canada (Fig. 1). We split the study area into several re-

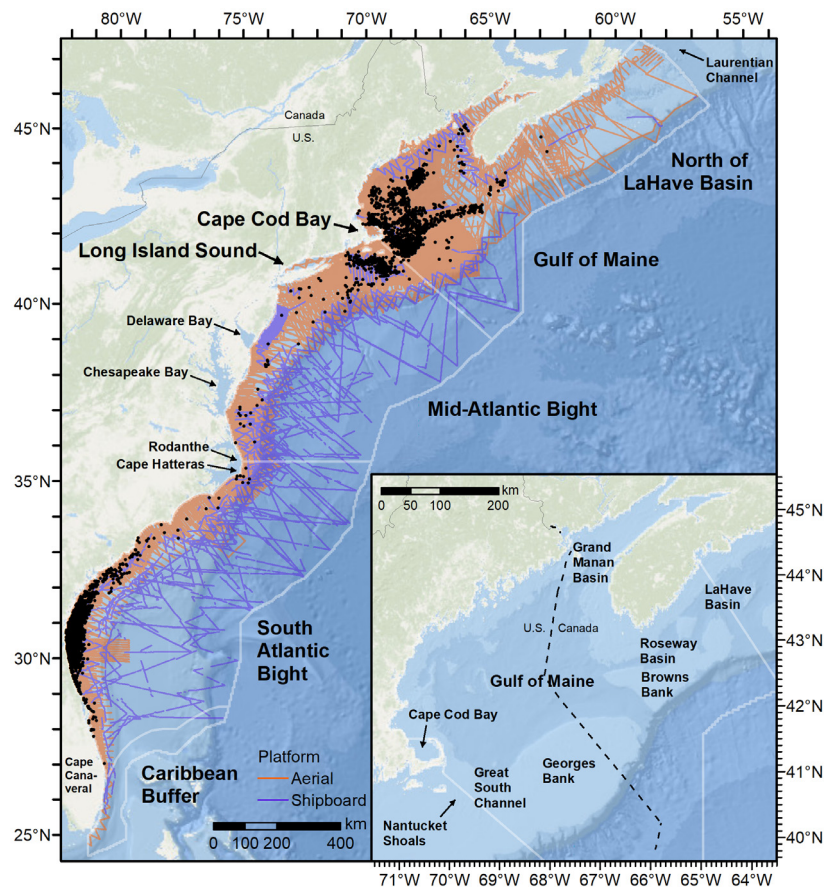


Fig. 1. Modeling regions (white-outlined polygons with large labels) with aerial transects (orange lines), shipboard transects (purple lines), and right whale sightings (black dots) available for modeling after detection functions were applied and excluded transects and truncated sightings were removed. Inset shows bathymetric features around the Gulf of Maine that are referenced in the text. Base map credits: Esri, Garmin, GEBCO, NOAA NGDC, and other contributors

gional models (see Section 2.2.4). We excluded Chesapeake Bay and Delaware Bay, where survey data were sparse and right whale sightings are very rare.

2.2. Density modeling

2.2.1. Detection modeling

For line-transect surveys, detection functions estimate the probability of detecting an animal given its perpendicular distance from the transect line as well as other conditions affecting detection probability, such as sea state. Ideally, at least 60–80 observations should be used to fit a detection function, but as few as 40 can be adequate (Buckland et al. 2001). With these guidelines in mind, we arranged the surveys available for our analysis into tree-like ‘detection hierarchies’ that grouped surveys according to the similarity in their detection characteristics (Roberts et al. 2016). We then traversed each hierarchy in a depth-first manner, intending to fit detection functions at the lowest-level nodes that pooled enough sightings to meet the 40–80 observations guideline. However, although long-running survey programs occasionally reported enough sightings to allow a detection function to be fitted for each annual survey, an exploratory analysis showed that this approach was inferior to a single detection function fitted for all years pooled together, especially when the pooled set allowed additional covariates to be utilized. When a branch of the hierarchy contained too few right whale sightings to fit an effective detection function, but it was not reasonable to ascend higher to obtain a larger pool of surveys, we included sightings of other large whale species in the pool (Barlow & Forney 2007, Palka et al. 2021). When sufficient sightings of each species were available, we tested the taxonomic identification as a covariate in the detection function to account for differences between species. Sightings of other species were used only in detection models; they were not used in the spatial models of right whale density described in following sections.

For each detection function (Supplementary Report Section 2), we attempted several formulations and selected the one with the lowest value of Akaike’s information criterion (AIC). We tested both conventional distance sampling using commonly recommended key functions and adjustment terms (Thomas et al. 2010) and multiple covariate distance sampling (Marques & Buckland 2003) using the sea state, other ocean and weather conditions, glare, the observer’s subjective estimate of the quality of observation con-

ditions, and the season as covariates. When data were combined from multiple survey programs, we tested the program, vessel, or aircraft used. For multi-year programs for which we had a specific reason to suspect interannual differences were not addressed by other covariates, we tested the year. We discarded covariates when the standard errors of their scale coefficients exceeded their estimates. We fitted all detection functions using the R package ‘mrds’ version 2.2.5 (Laake et al. 2021).

2.2.2. Bias correction

Distance sampling assumes that the detection probability is 1 for animals on the transect line (Buckland et al. 2001). When this assumption is not met and animals on the transect are missed, detection probability is biased high, leading to an underestimation of density. This problem is known as $g_0 < 1$, where g_0 refers to the detection probability at a perpendicular distance 0. Modelers often address this problem by estimating g_0 empirically and using this estimate to correct for the missed animals. Two important sources of bias that contribute to g_0 being < 1 for visual surveys are availability bias, in which an animal was present but impossible to detect (e.g. because it was underwater), and perception bias, in which an animal was available for detection but was not detected (e.g. because of its small size or cryptic coloration or behavior, or observer fatigue) (Marsh & Sinclair 1989). Modelers often estimate correction factors for these 2 biases independently (Hammond et al. 2021), hereafter referred to as g_{0A} and g_{0P} , and multiply them together to obtain a final, combined correction: $g_0 = g_{0A} \cdot g_{0P}$. We estimated g_0 on a per-sighting basis to account for differences in platform type (aerial vs. shipboard), institution, group size, group composition (e.g. singleton, mother–calf pair, or surface active group), and geographic location (Supplementary Report Section 3).

The only surveys conducted with protocols that permitted estimation of perception bias corrections were those from the NOAA AMAPPS program (Palka et al. 2021). These surveys used 2 independent teams on both shipboard and aerial platforms, allowing corrections to be estimated with mark–recapture distance sampling (Burt et al. 2014). We applied these corrections to all surveys, including those conducted by other institutions (having none better available for them). We caution that this could have biased our density estimates (see Section 4).

For aerial surveys, 92% of the sightings used to develop the AMAPPS corrections had a group size of

1 or 2 whales. For aerial sightings of 3 or more individuals, we assumed that perception bias was negligible (Carretta et al. 2000, Heide-Jørgensen et al. 2012, Hansen et al. 2018). We estimated availability bias corrections for aerial surveys using the availability model of Laake et al. (1997), accounting for aircraft speed and altitude, as well as right whale dive and surface intervals according to geographic location, group composition, and group size (Supplementary Report Section 3.1.2). Given that dive intervals were short relative to the amount of time a given patch of water remained in view to shipboard observers, we assumed that availability bias was negligible on shipboard surveys (Palka et al. 2021).

2.2.3. Preparation of segments and covariate grids for spatial modeling

We split survey transects into the segments that formed the data used to fit the spatial model using the method of Roberts et al. (2016), with a target segment length of 5 km. We discarded segments shorter than 1 km to avoid introducing high-leverage records into the data, representing a loss of 0.5% of the segments. Then, for each segment i , we computed the total number of individuals observed n_i , corrected by the sighting-specific bias correction:

$$n_i = \sum_r \frac{s_{ir}}{\hat{g}_{0ir}} \quad (1)$$

where s_{ir} is the group size reported for sighting r at the segment and \hat{g}_{0ir} is the estimated bias correction for the sighting. We then computed the effective area surveyed at the segment:

$$A_i = \left[\hat{p}_j(z_{iLEFT}) + \hat{p}_j(z_{iRIGHT}) \right] w_j l_i \quad (2)$$

where $\hat{p}_j(z_{iLEFT})$ is the probability of detection estimated by the survey's detection function j using the detectability covariates z_{iLEFT} for the left observer, and $\hat{p}_j(z_{iRIGHT})$ is the same for the right observer. w_j is the half-width of the segment (i.e. the detection function's right truncation distance minus left truncation distance, if any), and l_i is the length of the segment.

Based on input from NMFS and the US Navy, who planned to utilize the results in various management processes, and on the resolutions of available covariates, we set the model's spatial and temporal resolutions to 5 km and monthly. We assessed 21 spatial and environmental candidate covariates in the model (Table 1) that were plausibly correlated with cetacean habitat and available as gridded surfaces spanning

the entire study area in an uninterrupted time series from 1999–2020, with 25-km spatial resolution and monthly temporal resolution or higher. We favored products in which the covariate producer solved gap-filling problems, as with Level 4 remote sensing products. We resampled each product to the model's 5 km grid, filled any remaining gaps with a diffusion-based interpolation algorithm (D'Errico 2006, Crema et al. 2020), prepared monthly contemporaneous (per month, per year) and climatological (per month, all years) mean grids, and sampled both at each segment. We performed all processing in an Albers equal-area coordinate system.

2.2.4. Spatial modeling

The right whale's distribution shift, combined with life stage and regional complexity, raised fundamental challenges for the spatial model. One problem was that the population was distributed across several marine ecosystems at the same time, with whales in different locations exhibiting different environmental preferences. For example, whales that migrated to the warm, coastal calving grounds had different preferences than whales that overwintered in the cooler GOM. This complexity could be addressed by using spline smoothers, which allow for complex, non-linear relationships. However, the resulting multi-modal relationships would be difficult to interpret ecologically, which could impede qualitative evaluation of the models, and it was unclear whether a good result could be obtained without explicitly addressing the strong regional differences. Consequently, we split the study area into several regions (Fig. 1) within which we expected right whales to exhibit different relationships to environmental covariates and modeled each region separately (Roberts et al. 2016).

The 3 main regions of the model, the South Atlantic Bight (SAB), Mid-Atlantic Bight (MAB), and the GOM, correspond to the 3 distinct continental shelf ecosystems for which they are named plus the off-shelf waters adjacent to them. The SAB is strongly influenced by the Gulf Stream, a strong, warm, saline, subtropical, western boundary current that flows just beyond the eastern edge of the upper continental shelf (Seim et al. 2022). Evidence suggests that right whales rarely occupy the SAB outside of the winter calving season (Davis et al. 2017, Gowan et al. 2019). To ensure the SAB model spanned only the months that right whales were present, we restricted the model to the October–May period, based on reports of sightings or acoustic detections during those

Table 1. Candidate covariates for spatial modeling

| Type | Covariates | Resolution | Description |
|------------------------|--|---------------|---|
| Spatial | x, y | 5 km | Easting (m) and northing (m); geographic location in the projected coordinate system of the analysis |
| Static | Depth, Slope | 30 arc sec | Seafloor depth (m) and slope, derived from SRTM30-PLUS global bathymetry (Becker et al. 2009) |
| | DistToShore, DistTo125m, DistTo300m | 30 arc sec | Distance (km) to the closest shoreline, excluding Bermuda and Sable Island, and various ecologically relevant isobaths, derived from SRTM30-PLUS |
| | Fetch_50km | 30 arc sec | Mean distance (km) to shore averaged over 16 radial directions, limited to a maximum of 50 km |
| Physical oceanographic | SST_CMC | 0.2°, daily | Sea surface temperature (°C) from GHRSSST Level 4 CMC0.2deg and CMC0.1deg (Brasnett 2008, Meissner et al. 2016) |
| | DistToFront063, DistToFront105, DistToFront207 | 0.2°, daily | Distance to front in daily CMC_SST images detected with the edge detection algorithm of Canny (1986) with MGET (Roberts et al. 2010); 3 parametrizations tested |
| | BotT_HYCOM, SSS_HYCOM, BotS_HYCOM | 0.08°, 3 h | Bottom temperature (°C), and sea surface and bottom salinity (PSU), from the HYCOM GOFS 3.1 3-hourly ocean model (Chassignet et al. 2009) |
| | WindSpeed | 0.25°, 6 h | Wind speed (m s^{-1}) from the CCMP V2 L3 surface wind vectors (Atlas et al. 2011, Wentz et al. 2015) |
| Biological | Chl | 4 km, monthly | Chlorophyll a concentration (mg m^{-3}) from Copernicus GlobColour (Garnesson et al. 2019) provided by Copernicus Marine Service (CMEMS product code OCEANCOLOUR_GLO_CHL_L4_REP_OBSERVATIONS_009_082) |
| | PP_VGPM, PP_EVGPM, PP_CbPM, PP_CAFE | 4 km, monthly | Net primary productivity ($\text{mg C m}^{-2} \text{d}^{-1}$) from the Vertically Generalized Production Model (VGPM) (Behrenfeld & Falkowski 1997), 'Eppley' VGPM (Eppley 1972, Morel 1991), Carbon-based Production Model (CbPM) (Behrenfeld et al. 2005, Westberry et al. 2008), and Carbon, Absorption, and Fluorescence Euphotic-resolving (CAFE) model (Silsbe et al. 2016) |

months. During June–September, we assumed density in the SAB was zero.

At Cape Hatteras, the boundary between the SAB and the MAB, the Gulf Stream separates from the shelf and flows northeast into the North Atlantic. This area is an ecoregional boundary between distinct cetacean communities (Schick et al. 2011), where nutrient-rich, along-shelf currents flowing from the GOM south across the MAB turn east, cross the shelf, and merge with the Gulf Stream (Roarty et al. 2020). Although the MAB was not considered prime feeding habitat for right whales before 2010, since then they have been observed regularly feeding in SNE during all seasons (Quintana-Rizzo et al. 2021), and occasionally with open mouths (i.e. possibly feeding) at more southerly locations, such as off New York in May 2019 (Zoidis et al. 2021), New Jersey in January 2009 (Whitt et al. 2013), and Virginia in April 2018 (Engelhaupt et al. 2020). We placed the boundary between the SAB and MAB models slightly north of Cape Hatteras near Rodanthe, North Carolina, to

alleviate an edge effect that occurred when we placed it at Cape Hatteras itself. We modeled the MAB with a single, year-round model.

The GOM is a highly productive continental shelf sea around which the primary right whale feeding grounds were distributed until the 2010 shift. The GOM is isolated from the MAB to the south by the Nantucket Shoals and from the open Atlantic to the east by Georges Bank and Browns Bank (Townsend 1991). We placed the boundary between the MAB and GOM models at the northern edge of the Nantucket Shoals. The spatial extent of surveying in the GOM was seasonally variable; to accommodate this, we split the GOM model into 3 seasonal models with varying spatial extents. At its largest extent, in 'summer' (August–September), the modeled region extended north to LaHave Basin offshore of Nova Scotia. North of LaHave, survey effort was too sparse and heterogeneous to obtain reasonable model predictions, so we did not model it. In 'winter' (October–February), the region extended to the US–Canada

border, as virtually no visual surveying occurred in Canada at this time. In 'spring' (March–July), the model extended slightly farther, encompassing the entirety of Georges Bank.

CCB is an important feeding ground where right whales reliably aggregate in high numbers from January to May (Mayo et al. 2018, Ganley et al. 2019). CCB has been surveyed extensively by the Center for Coastal Studies (CCS) for more than 2 decades, but until recently, CCS did not collect distances to sightings, making the data unusable for our model. Instead, for December–May, we derived per month, per year, CCB-wide density estimates from the abundance estimates of Ganley et al. (2019) and subsequent data from CCS (Supplementary Report Section 4.4). For June–November, we included CCB in the GOM model or assumed density was zero, depending on the month. Finally, during all months, we assumed density was zero in Long Island Sound and the 'Caribbean Buffer' (Fig. 1). These are poor right whale habitats, and the surveys in our analysis reported no sightings there, but we caution that opportunistic sightings have occurred very occasionally.

Another fundamental problem in modeling the right whale distribution was its strong temporal variability, which included seasonal variations related to the species' life cycle, interannual variations associated with shifting prey availability, and the long-term rise and fall in the population and its health. Compounding this challenge and limiting our ability to address it were strong seasonal and interannual variations in survey effort across most of the study area. Our approach was first to assume that the significant interannual changes in the distribution were not related to changes in right whale environmental preferences but rather that the environment had changed, and the whales redistributed in response. Therefore, rather than fitting different models to different eras, such as 2003–2009 and 2010–2020, we fitted a single model to the entire period and relied on contemporaneous dynamic environmental covariates, resolved to the year and month, to address interannual changes in distribution. Because we lacked potentially important covariates such as prey density, we also included either the year or the era (e.g. 2003–2009 and 2010–2020) as categorical covariates, depending on the degree of interannual replication in survey effort, to account for unexplained interannual variability in regional abundance.

We also relied on dynamic environmental covariates to address seasonal changes. However, in the GOM, where right whale movements were particularly complex and challenging to resolve with a sin-

gle, year-round model and the spatial extent of survey effort depended strongly on the season, we split the year into the 3 seasonal models discussed above and included interactions between day of year and distance to CCB as covariates, to better capture their annual cycling around the GOM (Kenney et al. 2001, Brillant et al. 2015). We did not explicitly incorporate the known population decline or health effects (e.g. the influence of anthropogenic stressors on movement patterns; Schick et al. 2013) in the model.

After defining the regions, we fitted log-link GAMs for each of the SAB, MAB, and 3 seasonal GOM regions:

$$\mathbb{E}(n_i) = A_i \exp \left[\beta_0 + \sum_k f_k(z_{ik}) \right] \quad (3)$$

where the segment's effective area A_i is an offset, β_0 is an intercept, and each $f_k(z_{ik})$ is a smoothed function of the spatial model covariate k with the value z_{ik} for the segment. We fitted GAMs in R with the 'mgcv' package version 1.8-36 (Wood 2017). We used thin-plate regression splines with shrinkage smoothers (Marra & Wood 2011), the Tweedie distribution (Miller et al. 2013) with automatic selection of the power parameter, and restricted maximum likelihood (REML; Wood 2011) for smoothness selection. If a covariate p-value was >0.05 or its estimated degrees of freedom were <0.85 , we removed the covariate from the model and refitted it.

For each GAM, we fitted and ranked a large number of candidate models that utilized different combinations of covariates. We lacked the computing capacity to try all possible combinations of covariates, so we used the 2-step procedure of Roberts et al. (2023) to first identify a smaller number of the most promising covariates and then tested all combinations of those. We used contemporaneous formulations of covariates except in the GOM summer model, for which interannual replication in surveying was very sparse and climatological formulations yielded better results (Supplementary Report Section 4.3.3). We ranked candidates by REML score, inspected predictions, and selected one as best. This selection was informed by the candidates' statistical performance, the spatiotemporal noisiness of the predictions, and our judgment of how well the predictions matched well-established findings from the literature (detailed discussion and diagnostic plots in model-specific subsections of Section 4 in the Supplementary Report). We also assessed the degree of univariate and multivariate extrapolation across model covariates using the NT1 and ExDet statistics (Mesgaran et al. 2014, Bouchet et al. 2020), and either avoided covariates for

which excessive extrapolation occurred or Winsorized relationships (Dixon 1960), rounding extreme values up or down to well-sampled ranges to avoid such extrapolation without discarding the out-of-range records. When these checks did not reveal important concerns among the top candidate models, we selected the model with the lowest REML score.

2.2.5. Model prediction and summarization

After selecting the final models for each region, we used them to predict right whale density across the overall study area and time period (October 2003–September 2020). For species management purposes, NOAA and the US Navy requested we summarize the results into monthly mean density surfaces. To characterize and account for the major shift in distribution that occurred around 2010, we prepared separate monthly summaries for the 2003–2009 and 2010–2020 periods (Supplementary Report section 5.1). To summarize uncertainty, we estimated empirical variance with a method that accounted both for interannual variability in dynamic covariates and for uncertainty in model parameter estimates (Miller et al. 2022), except in the case of the GOM summer model (August–September) for which climatological covariates were used and thus interannual variability was not accounted for. For each monthly mean density surface, we produced a standard error (SE) and coefficient of variation (CV) surface which depicted the variability that would result if a single random year within the summary period was selected instead of the multi-year mean.

2.3. Evaluation of density predictions with PAM

PAM detections represent a source of right whale distribution data to which our density predictions can be compared for validation purposes. For some species, density may be estimated from vocalizations detected by fixed PAM sensors, so long as vocalization rates can be accurately determined and the relationship between detection probability and distance to the sensor can be characterized (Marques et al. 2013). For right whales, which are highly variable callers, neither of those problems had been solved, so it was not possible to derive right whale density from PAM detections for direct comparison. As an alternative, we estimated the rate of acoustic presence as the number of days per month having detected vocalizations, using in this case the upcall, a reliable right whale vocalization produced across regions by all ages and sexes

(Davis et al. 2017). Under the assumption that this metric should correlate with density, we obtained daily acoustic presence data from recorders deployed within our study area (Davis et al. 2017 and their additional unpublished data) and summarized them into monthly rates of daily presence resolved to the months of the years the recorders were deployed (2004–2020). That is, for each month of each year during which a recorder was deployed, we divided the number of days that whales were acoustically present (as determined with the method of Davis et al. 2017) by the number of days that were monitored. We caution that non-vocalizing animals might still have been present when no acoustic activity was recorded (Delarue et al. 2022), and that calling whales might have been missed when occurrence was very low and very few calls were available for detection. When a recorder was monitored on fewer than 5 days of a month of a year, we dropped that month of that year of that recorder from the analysis. We then assessed the correlation between acoustic presence rate and the density estimated at that location and time using Pearson's correlation coefficient (r) and locally estimated scatterplot smoothing (LOESS, Cleveland & Devlin 1988). Because the resulting smoothed relationship was nonlinear (see Fig. 8), we also assessed the correlation with Spearman's (ρ) and Kendall's (τ) rank correlation coefficients. Finally, for visual comparison, we overlaid the recorders on summarized density maps, symbolizing the recorders by monthly acoustic presence rate. To preserve the value of the acoustic data as an independent source of right whale distribution data to which density predictions could be compared, we did not develop any of the comparative maps or statistics until after the density models were finalized. However, *a priori* knowledge of acoustic findings (e.g. Davis et al. 2017) was impossible to exclude from qualitative assessments of candidate models; therefore, the models are not wholly independent from the acoustic data.

3. RESULTS

3.1. Survey data

In total, the collaborating survey institutions contributed 2914 000 km of line-transect survey effort, comprising 9786 000 km² of effective effort once detection functions were applied (Table 2, Fig. 1), roughly the same as the land area of the USA. The surveys sighted 4439 groups, comprising 13 565 individuals. Aerial surveys accounted for 2 835 000 km (97%) of the effort and 4374 (99%) of the sightings. On an

Table 2. Survey programs and data used in this analysis. Effort is expressed as linear distance traversed and effective area surveyed after detection functions were applied and excluded transects removed. Sightings reported both as groups and individuals; elsewhere in this article, sightings are always reported as groups. Institutions: FWRI: Florida Fish and Wildlife Conservation Commission (FWC) Fish and Wildlife Research Institute; HDR: HDR, Inc.; NEAq: New England Aquarium; NEFSC: National Oceanographic and Atmospheric Administration (NOAA) Northeast Fisheries Science Center; NJDEP: New Jersey Department of Environmental Protection; MCR: Marine Conservation Research; NYS-DEC/TT: New York State Department of Environmental Conservation and Tetra Tech, Inc.; SEFSC: NOAA Southeast Fisheries Science Center; UNCW: University of North Carolina Wilmington; VAMSC: Virginia Aquarium & Marine Science Center; WLT/SSA/CMARI: Wildlife Trust/Sea to Shore Alliance/Clearwater Marine Aquarium Research Institute. Survey program names and citations are given in the Supplementary Report Section 1

| Institution | Program | Period | Effort | | Sightings | |
|--------------------------|---------------------|--------------------|-------------|-----------------------|-------------|--------------|
| | | | 1000s km | 1000s km ² | Groups | Individuals |
| Aerial surveys | | | | | | |
| FWRI | SEUS NARW EWS | 2003–2020 | 668 | 2609 | 806 | 2,305 |
| HDR | Navy Norfolk Canyon | 2018–2019 | 11 | 22 | 2 | 8 |
| NEAq | CNM | 2017–2020 | 2 | 5 | 0 | 0 |
| NEAq | MMS-WEA | 2017–2020 | 37 | 91 | 109 | 453 |
| NEAq | NLPSC | 2011–2015 | 43 | 118 | 37 | 122 |
| NEAq | SEUS NARW EWS | 2003–2010 | 227 | 1137 | 926 | 2489 |
| NEFSC | AMAPPS | 2010–2019 | 89 | 94 | 18 | 27 |
| NEFSC | NARWSS | 2003–2020 | 484 | 2199 | 1571 | 5917 |
| NEFSC | Pre-AMAPPS | 1999–2008 | 46 | 94 | 29 | 39 |
| NJDEP | NJEBS | 2008–2009 | 11 | 9 | 0 | 0 |
| NYS-DEC/TT | NYBWM | 2017–2020 | 77 | 163 | 12 | 19 |
| SEFSC | AMAPPS | 2010–2020 | 114 | 117 | 6 | 13 |
| SEFSC | MATS | 2004–2005 | 13 | 11 | 4 | 9 |
| UNCW | Navy Cape Hatteras | 2011–2017 | 34 | 38 | 0 | 0 |
| UNCW | Navy Jacksonville | 2009–2017 | 92 | 103 | 2 | 3 |
| UNCW | Navy Norfolk Canyon | 2015–2017 | 14 | 16 | 0 | 0 |
| UNCW | Navy Onslow Bay | 2007–2011 | 49 | 55 | 0 | 0 |
| UNCW | SEUS NARW EWS | 2005–2008 | 114 | 67 | 18 | 37 |
| VAMSC | MD DNR WEA | 2013–2015 | 16 | 16 | 5 | 13 |
| VAMSC | Navy VACAPES | 2016–2017 | 19 | 22 | 2 | 2 |
| VAMSC | VA CZM WEA | 2012–2015 | 21 | 24 | 5 | 8 |
| WLT/SSA/CMARI | SEUS NARW EWS | 2003–2020 | 652 | 2492 | 822 | 2000 |
| | | Total | 2835 | 9504 | 4374 | 13464 |
| Shipboard surveys | | | | | | |
| MCR | SOTW Visual | 2012–2019 | 9 | 13 | 0 | 0 |
| NEFSC | AMAPPS | 2011–2016 | 16 | 78 | 20 | 31 |
| NEFSC | Pre-AMAPPS | 1999–2007 | 9 | 26 | 42 | 66 |
| NJDEP | NJEBS | 2008–2009 | 14 | 56 | 2 | 3 |
| SEFSC | AMAPPS | 2011–2016 | 17 | 73 | 1 | 1 |
| SEFSC | Pre-AMAPPS | 2004–2006 | 15 | 37 | 0 | 0 |
| | | Total | 79 | 282 | 65 | 101 |
| | | Grand total | 2914 | 9786 | 4439 | 13565 |

annual basis, the highest effort occurred during 2004–2012, after which effort declined steadily (Fig. 2A). The most sightings were reported during 2007–2010 (Fig. 2C), reflecting both the high level of survey effort and the peak population size. In addition, many whales migrated to the calving grounds during those years (Gowan et al. 2019), where effort was concentrated. Effort and sightings were highest during December–March (Fig. 2B,D), when most of the population was likely in US waters and surveys covered the calving grounds several times per month. Effort and sightings were lowest during August–

October, when much of the population was likely in Canada (or farther afield) and our collaborators reduced their survey effort.

3.2. Density models

3.2.1. Detection models

We fitted 20 detection functions (Supplementary Report Section 2). Of these, 6 were specific to right whales, for the long-running right whale aerial survey

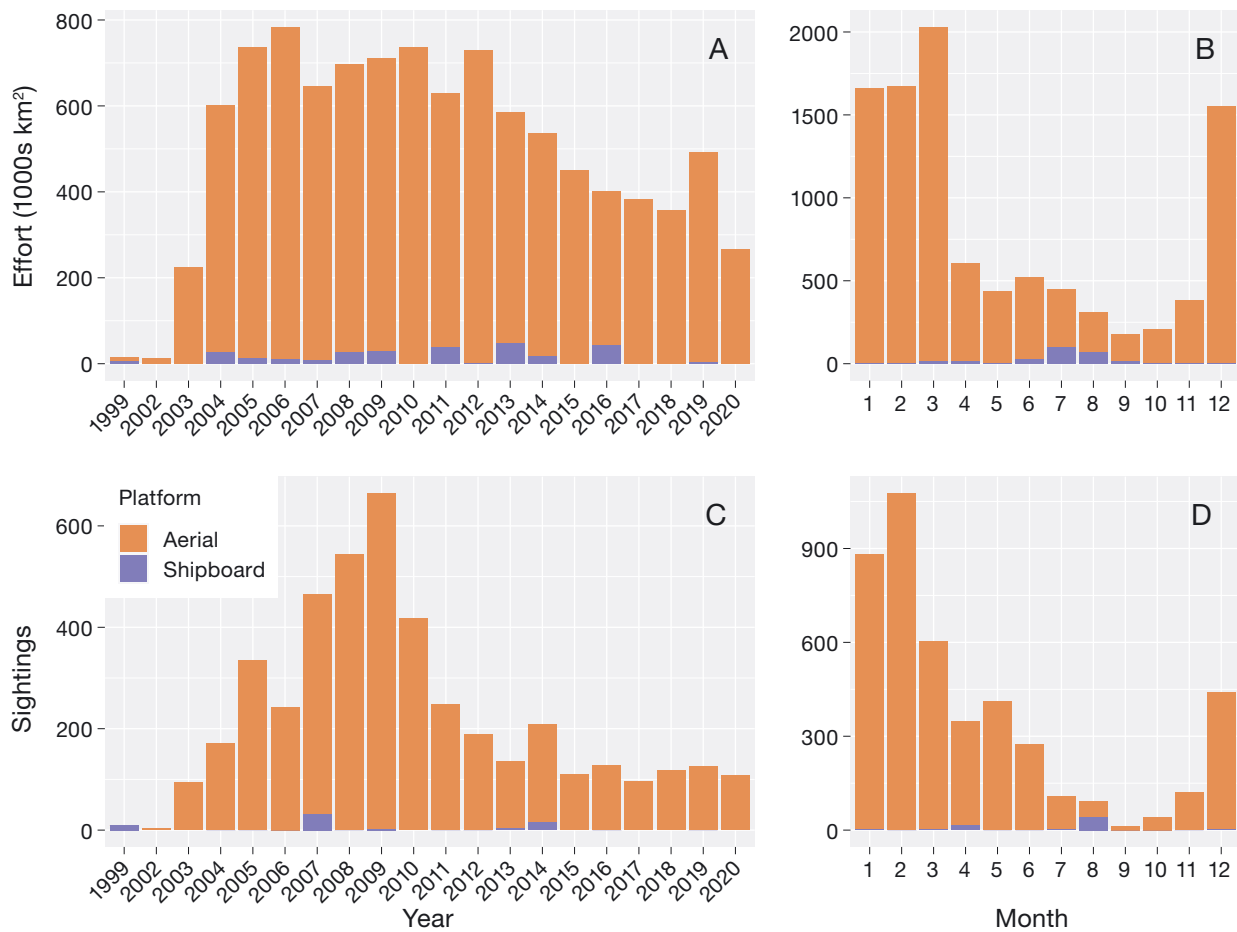


Fig. 2. (A,B) Effective effort and (C,D) sightings, by year (A,C) and month (B,D)

programs in the US Northeast and Southeast. Another 14 incorporated sightings of other large whale species to increase sighting counts. Among them, 8 used a taxonomic covariate to account for detectability differences between the species. The remaining 6 detection functions, for programs that covered low-density areas, did not have sufficient sightings to account for species detectability differences. Across all detection functions, mean effective strip half-widths (transect half width w multiplied by estimated detection probability \hat{p}) ranged from 321 m for an aerial survey focused on bottlenose dolphins to 2710 m for NOAA shipboard marine mammal surveys that utilized 25×150 'bigeye' binoculars.

3.2.2. Spatial models

Final model formulations, diagnostics, and detailed commentary for each model appear in the Supplementary Report as noted below; here, we summarize

overall outcomes. Survey effort was strongly biased toward the SAB region, reflecting the long-term, consistent high level of effort by the Southeast right whale EWS survey programs. As a result, the SAB model (Supplementary Report Section 4.1) had about twice as much effort and 40% more sightings than the other models combined (Table 3). The MAB model (Supplementary Report Section 4.2) had the second-largest quantity of effort but the lowest sightings per unit effort, with most of the sightings occurring in SNE. In the GOM region (Supplementary Report Section 4.3), effort was biased toward spring (March–July), when right whales were most frequent in the region, and the number of sightings per unit effort was the highest across the 5 spatial models. Effort during summer (August–September), when most whales had migrated to Canadian waters, was sparse, but it was the only season with substantial coverage in Canada.

All regions benefited from the inclusion of temporal covariates that accounted for interannual or seasonal

Table 3. Summary of final spatial models. Seasons were region-specific and defined to accommodate patterns in right whale distribution and survey effort. Complete details for each model are given in the Supplementary Report Section 4. SAB: South Atlantic Bight; MAB: Mid-Atlantic Bight; GOM: Gulf of Maine

| Region | Season | Months | Effort | | | | Temporal covariates | % Deviance Explained |
|--------|------------|------------------|----------|----------|-----------------------|-----------|---------------------|----------------------|
| | | | Segments | 1000s km | 1000s km ² | Sightings | | |
| SAB | Winter | October–May | 370942 | 1754 | 6521 | 2564 | Year | 16.0 |
| MAB | Year-round | January–December | 120643 | 530 | 1268 | 412 | Era | 39.4 |
| GOM | Winter | October–February | 26415 | 132 | 680 | 317 | DayOfSeason | 39.5 |
| GOM | Spring | March–July | 52842 | 264 | 1130 | 1031 | Era, DayOfYear | 27.8 |
| GOM | Summer | August–September | 12807 | 63 | 157 | 74 | Era | 67.6 |

variations not fully explained by the candidate environmental covariates (Table 3). In the SAB, consistent interannual replication of effort at the calving grounds from December–March allowed us to include Year as a categorical covariate to address high interannual variability in right whale abundance, which has been linked to prey abundance in the GOM during previous summers (Gowan et al. 2019), while SST was a strong correlate with seasonal variability (Keller et al. 2012, Gowan & Ortega-Ortiz 2014). In the MAB, which lacked a long-term dedicated survey program spanning the region, interannual replication was patchy and dependent on smaller-scale programs that usually operated for only a few years. Because of this, we included a categorical ‘Era’ covariate with 2 levels, 2003–2009 and 2010–2020, to account for the strong increase in usage of the SNE area in the latter era (Quintana-Rizzo et al. 2021, O’Brien et al. 2022). Seasonal variability was addressed by SST and a primary productivity covariate. The GOM received better interannual replication in winter and spring, but we judged that effort was still too heterogeneous to include a Year covariate, so we tested an Era covariate. In winter, Era was not statistically significant and was discarded; in spring, it was retained but a much weaker effect was estimated than in the MAB model. These outcomes indicate the environmental covariates had greater interannual predictive power in the GOM than in the MAB. Both seasons benefited from including Day of Season or Day of Year as a continuous interaction term with the distance to CCB to account for seasonal movement across the GOM not explained by the environmental covariates. In summer, interannual replication in effort was very sparse but sufficient to include an Era covariate, which exhibited a strong effect, reflecting the substantial decline in the use of traditional Canadian feeding grounds at Grand Manan Basin and Roseway Basin starting in 2010 (Davies et al. 2019, Record et al. 2019, Meyer-Gutbrod et al. 2021). With the summer

season being only 2 mo long, there was no benefit to including a temporal covariate to capture unexplained seasonal variability.

The SAB model explained the least deviance in the data (16%), reflecting the patchy distribution of whales within the core calving habitat where the survey effort was focused. Models for the other regions explained more deviance (Table 3), suggesting the covariates better tracked seasonal movements and interannual variability. The GOM summer model explained the most deviance (67.6%) but was only 2 mo long, so seasonal variability was not a concern; the Era covariate addressed the extreme inter-era decrease in density.

3.2.3. Predictions

To characterize mean density and how it changed before and after the distribution shifted in approximately 2010, we summarized predictions into 3 eras: 2003–2009 (spanning October 2003–September 2010), 2010–2019 (October 2010–September 2020), and 2003–2019 (October 2003–September 2020). We summarized October–September rather than January–December because it better matched the start and end dates of the survey data. Here, we present one monthly map from the 4 meteorological seasons from the 2003–2019 era as exemplars (maps for all months of all eras in Supplementary Report Section 5.1).

In February, the population was dispersed across the study area, with whales aggregated at the calving grounds, SNE, the western GOM, and CCB, and scattered across the MAB and northern SAB (Fig. 3). In May, the population had largely vacated the SAB and much of the MAB, but remained present in moderate densities in SNE (Fig. 4). The highest densities were predicted in the Great South Channel (GSC), an important spring foraging area (Kenney et al. 1995),

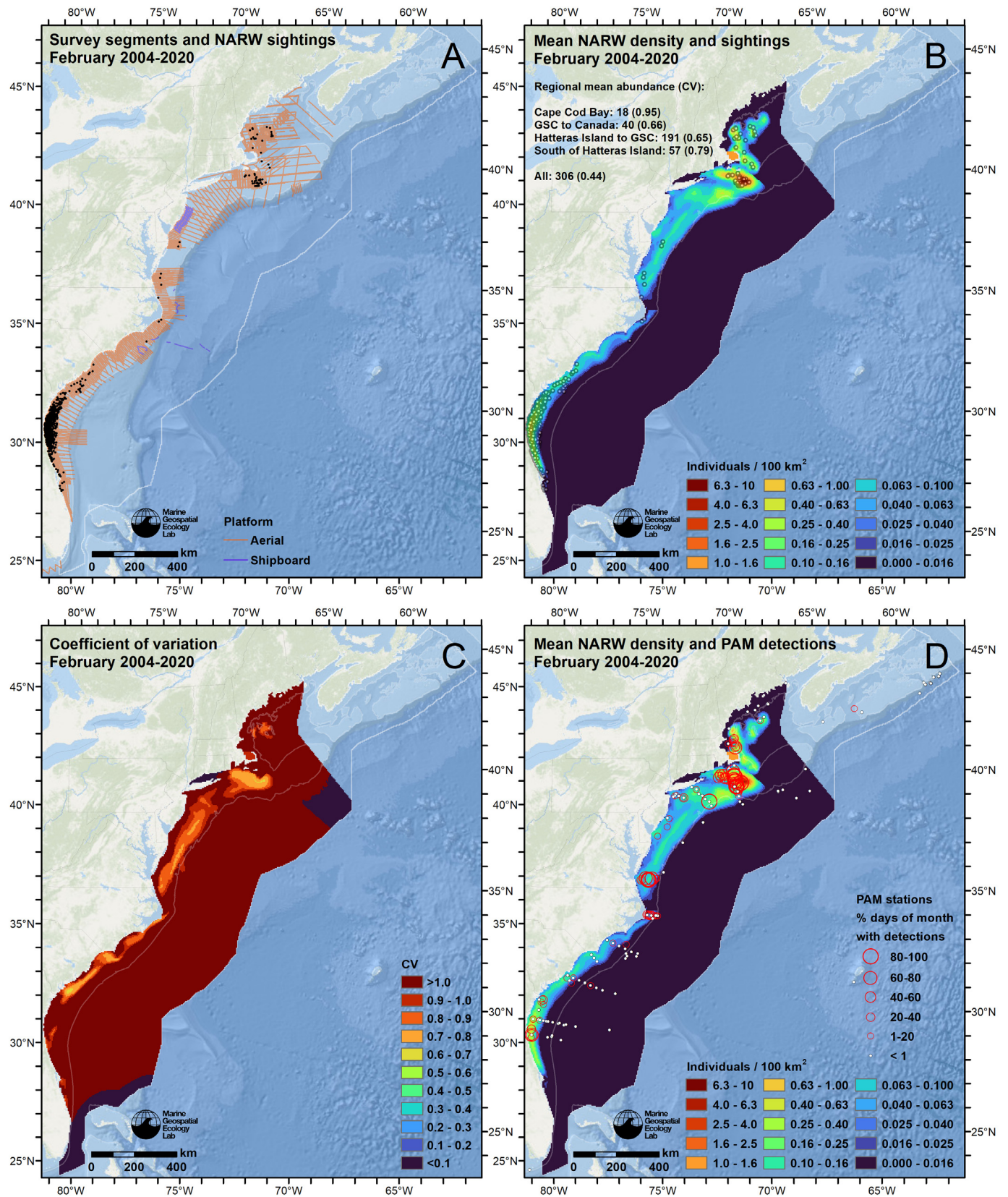


Fig. 3. (A) Survey segments and right whale sightings, (B) mean predicted density with sightings overlaid, (C) coefficient of variation, and (D) density with passive acoustic monitoring (PAM) detection rates overlaid for February 2004–2020. Base map credits: Esri, Garmin, GEBCO, NOAA NGDC, and other contributors

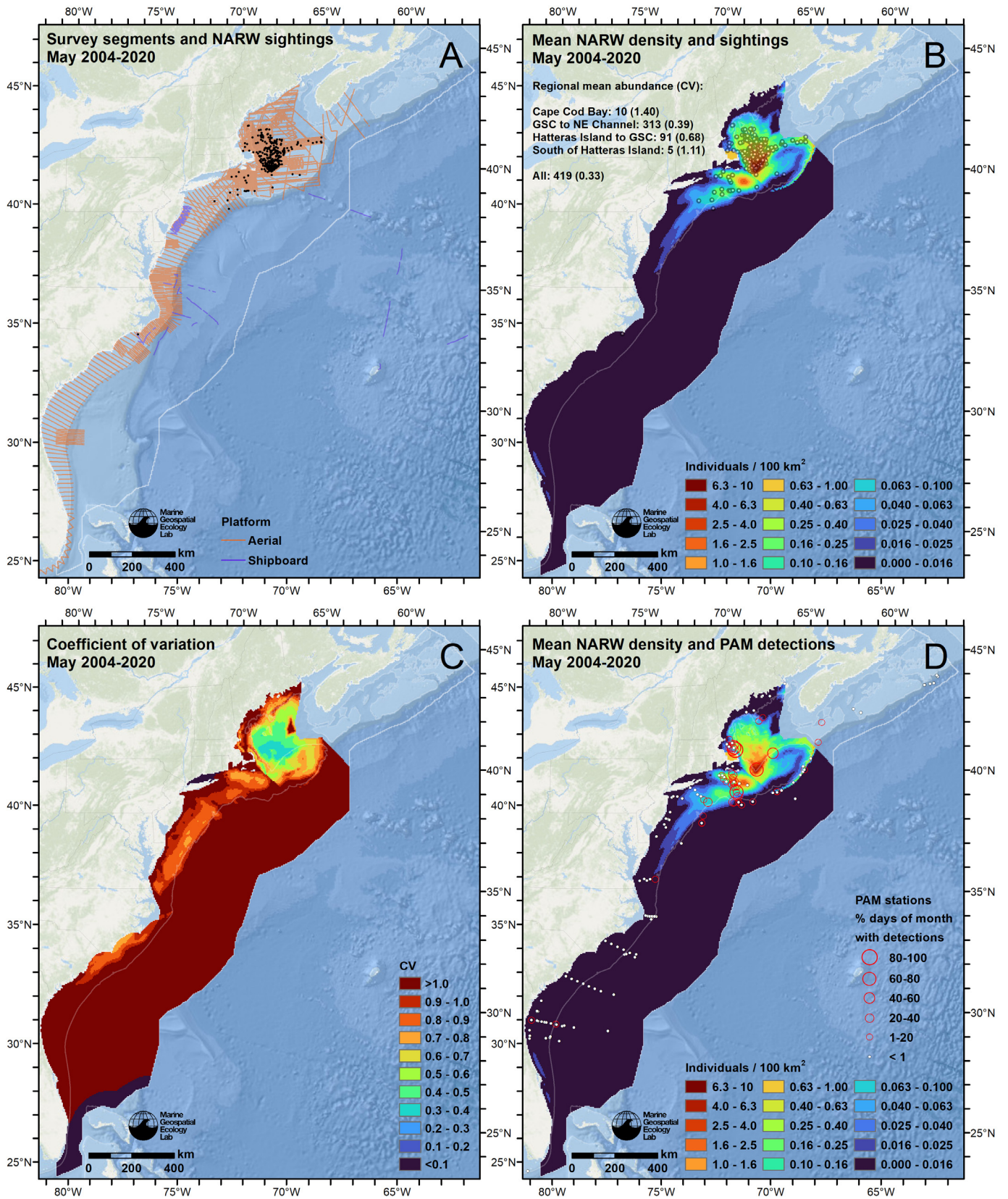


Fig. 4. As in Fig. 3, but for May 2004–2020

as the population moved east out of CCB and north from SNE. In August, density was concentrated in Canada, particularly at Roseway Basin and Grand Manan Basin (Fig. 5), both important summer feeding grounds during the 2000s (Davies et al. 2015), while the only appreciable density predicted in US waters was in SNE and along the 125 m isobath from Maine through Cape Cod. In November, density was concentrated in the western GOM (Cole et al. 2013) and increased from summer in SNE and the calving grounds, as whales began to return from summer feeding grounds (Fig. 6).

Density differences between the 2003–2009 and 2010–2019 eras were substantial in all regions, with strong decreases in the SAB and GOM and strong increases in the MAB and CCB (Fig. 7). Across the 4 months presented, prediction uncertainty across the 2003–2019 era (Figs. 3C–6C) was moderate to high ($CV > 0.5$), reflecting both the strong inter-era differences as well as within-era interannual variability. Uncertainty within the 2003–2009 and 2010–2019 eras individually, which excluded the large inter-era differences, was lower (Supplementary Report Section 5.1).

3.2.4. Comparison to PAM

NMFS NEFSC, using PAM data contributed by a large collaboration (Davis et al. 2017 and their subsequent unpublished data), provided daily acoustic presence data at 492 recorders deployed between August 2004 and September 2020 (mean duration = 138 d). We summarized these into 2518 records of the monthly rate of daily acoustic presence at a given recorder, year, and month. (We discarded a further 152 records that had fewer than 5 d of recording.) Correlation analysis revealed positive correlations between our model's predicted density and monthly acoustic presence rate (Fig. 8), with the highest correlation in the MAB ($r = 0.56$, $\rho = 0.65$, $\tau = 0.50$) and lowest in the SAB ($r = 0.40$, $\rho = 0.47$, $\tau = 0.38$). Monthly correlation statistics for the 2010–2019 era indicated higher correlations during November–June with a notable decrease during July–October (Fig. 9).

4. DISCUSSION

4.1. Predicted right whale distribution

Our predicted monthly mean density surfaces largely resembled the distribution patterns described

in the literature, with whales migrating south into the MAB during November–December, aggregating in the SAB during December–March (while some overwintered in the MAB and GOM), departing the SAB and southern MAB during April–June, and cycling counterclockwise annually around the GOM (e.g. Kenney et al. 2001, Gowan & Ortega-Ortiz 2014, Bril-lant et al. 2015, Leiter et al. 2017, Quintana-Rizzo et al. 2021). Strong differences between the 2003–2009 and 2010–2019 eras were predicted (Fig. 7). In the SAB, mean density predicted for January–April declined strongly from 2008 to 2018 before rebounding slightly in 2020 (Supplementary Report Fig. 164), generally mirroring the interannual trend in calf counts (Pettis et al. 2023). In the MAB, density was an order of magnitude higher during the 2010–2019 era than 2003–2009, with the greatest increase in SNE, particularly in winter and spring, consistent with the strong increase in sightings and acoustic detections there (Davis et al. 2017, Quintana-Rizzo et al. 2021, O'Brien et al. 2022). In the GOM, density was lower during the 2010–2019 era in all seasons, consistent with prior findings, especially in important feeding areas such as the GSC in spring and Grand Manan Basin and Roseway Basin in summer (Davies et al. 2019, Record et al. 2019, Meyer-Gutbrod et al. 2021, 2023). Density also declined in fall and winter in the northwestern GOM, consistent with acoustic results (Davis et al. 2017), but we caution that visual surveying of this area decreased strongly during 2016–2020, limiting the model's ability to detect density changes. We recommend that surveying in this area be restored to the level it was in 2008–2015.

4.2. PAM

In this analysis, we observed positive correlations ($r = 0.46$, $\rho = 0.58$, $\tau = 0.46$) between acoustic right whale presence rate and predicted right whale density across a database of nearly 500 PAM deployments. This correspondence supports the density predictions, but we caution that this analysis did not address heterogeneity in the spatiotemporal distribution of PAM sensors, so the estimated correlations may not be unbiased.

The analysis revealed both regional and seasonal differences. However, right whales produce many vocalizations other than upcalls and exhibit variable calling rates and behavior in different regions and during different activities (Franklin et al. 2022), for which we lacked the data to take into account. Our correlations were weakest in the SAB, and the LOESS regression

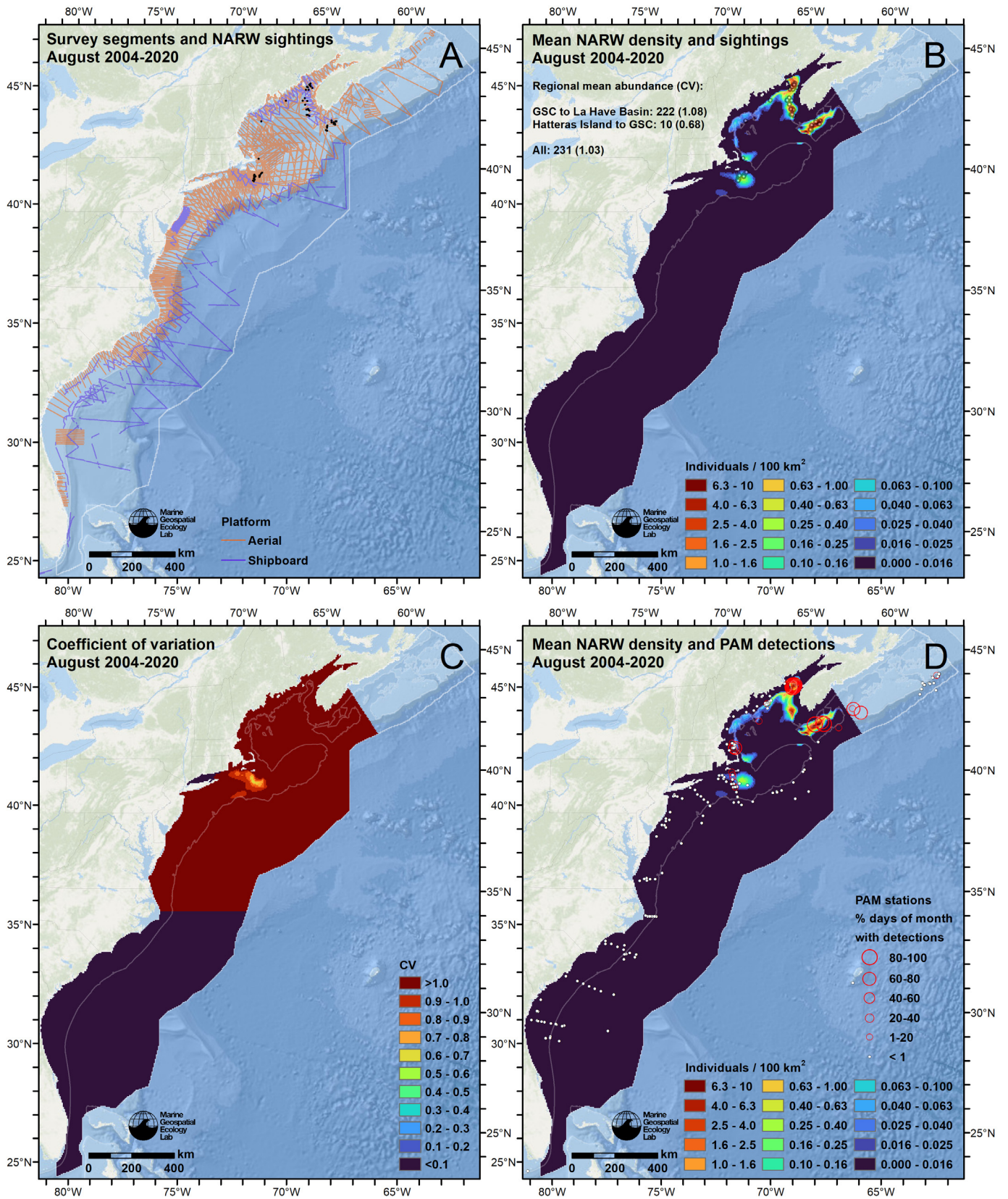


Fig. 5. As in Fig. 3, but for August 2004–2020

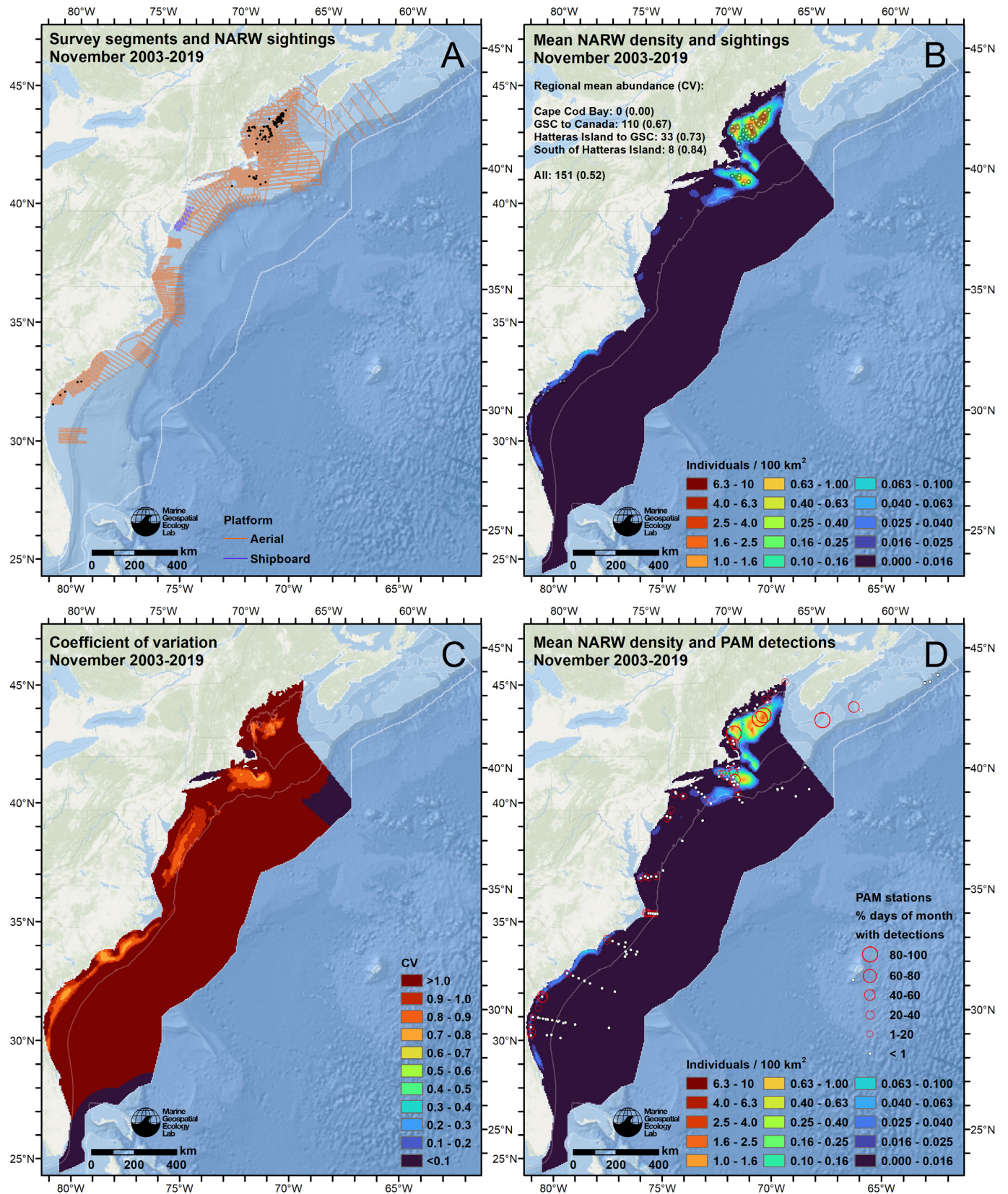


Fig. 6. As in Fig. 3, but for November 2003–2019

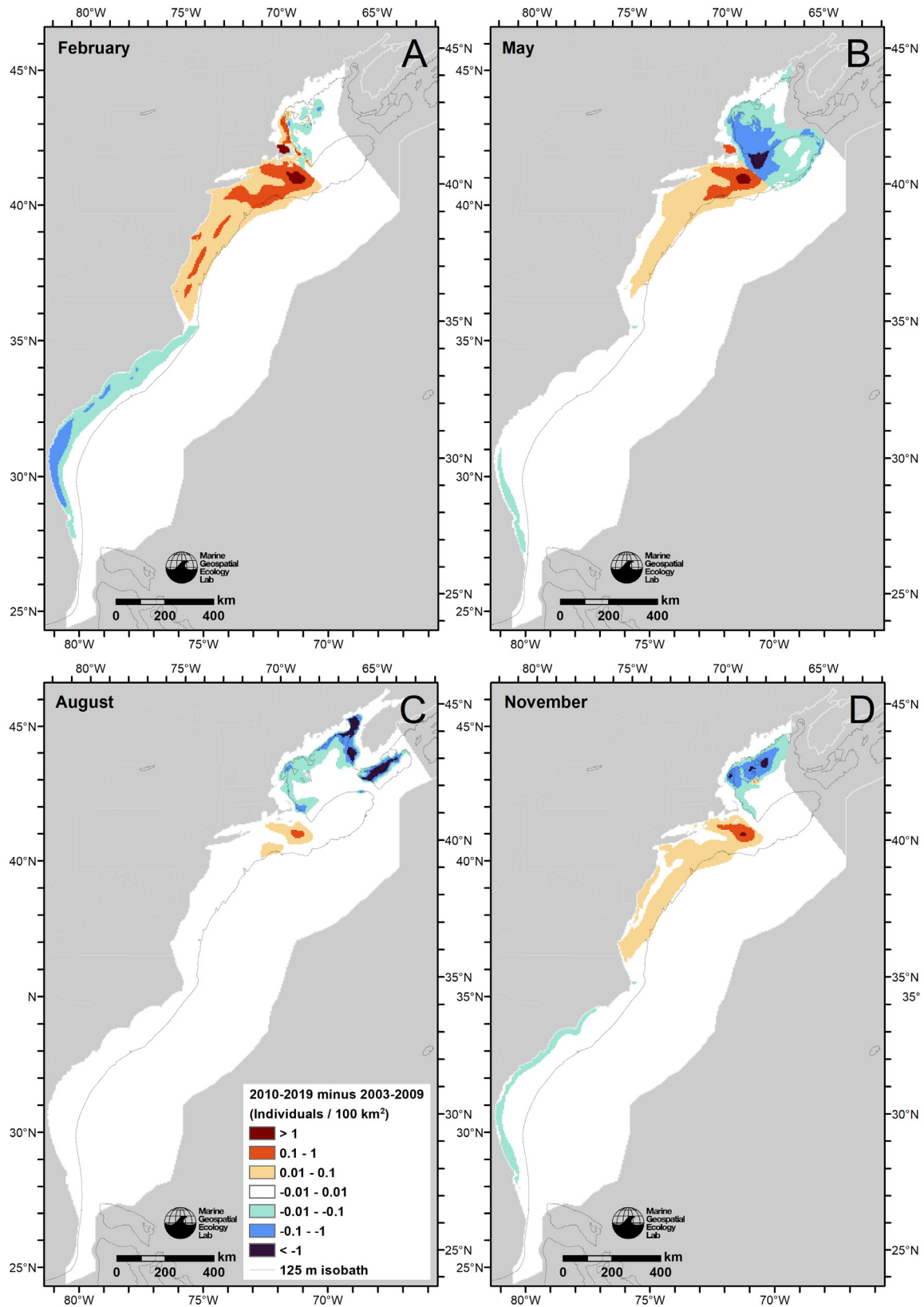


Fig. 7. Differences in mean monthly densities predicted for the 2010–2019 and 2003–2009 eras for (A) February, (B) May, (C) August, and (D) November. Red indicates density was higher in 2010–2019; blue indicates density was lower in 2010–2019; white indicates density was about the same

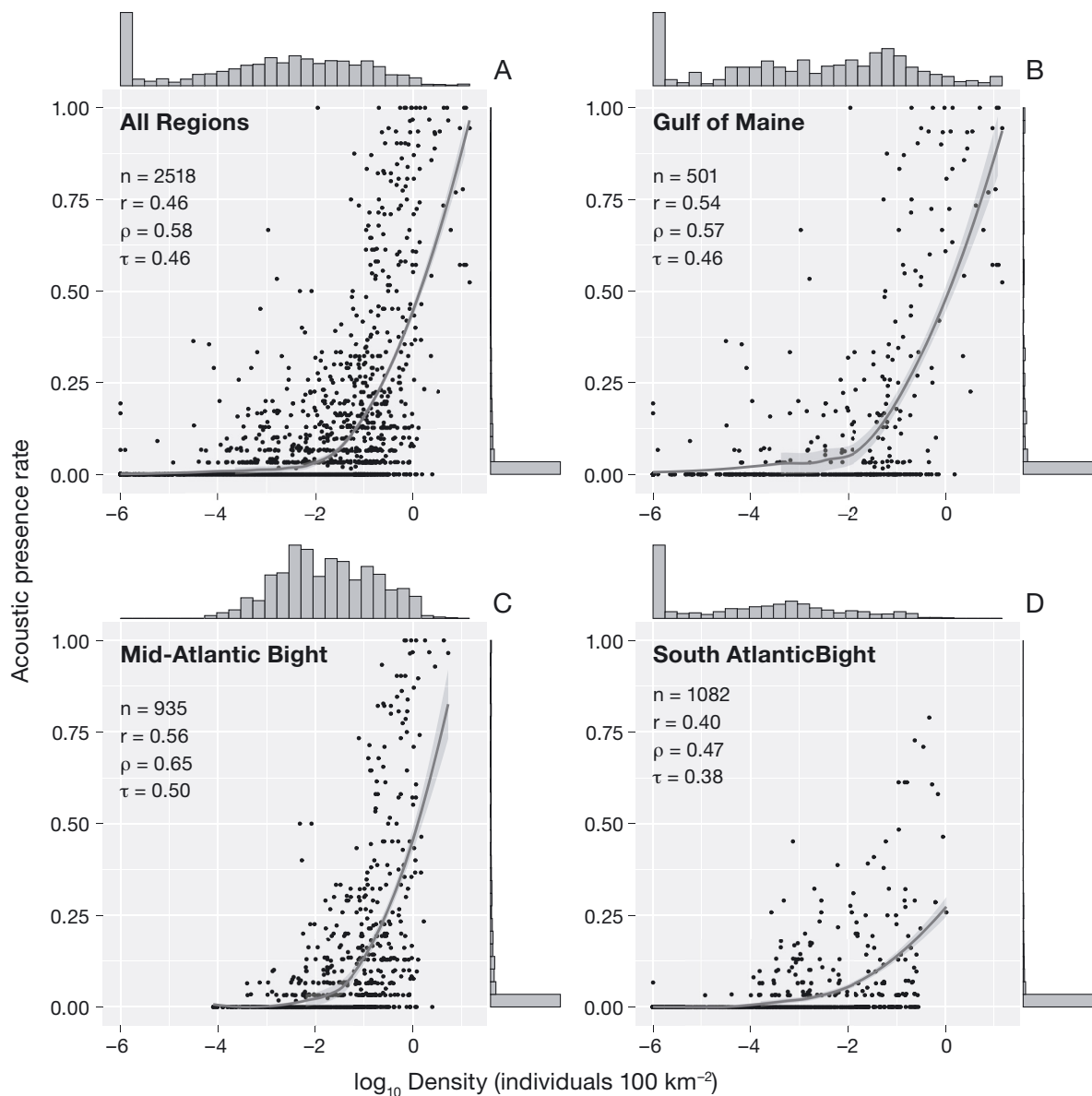


Fig. 8. Monthly rate of daily acoustic presence vs. predicted density, by region, for passive acoustic monitoring recorders deployed 2004–2020. Each point represents a month during which a recorder was deployed for at least 5 d. Pearson's r , Spearman's ρ , and Kendall's τ correlation coefficients and a LOESS curve assess the strength of correlation. Density values $< 10^{-6}$ were rounded up to 10^{-6} to improve visualization after the statistics were calculated. Horizontal and vertical histograms show the distributions of density values and acoustic presence rates, respectively, for the points within each plot

was much flatter there, indicating lower acoustic presence at high predicted densities. The proportion of aerial sightings utilized in the SAB model that were mother–calf pairs was 47%, much greater than in the other regions. Mother–calf pairs on the calving grounds exhibit significantly fewer higher-amplitude, long-distance communication signals than juvenile and pregnant whales (Parks et al. 2019). This life-history specific vocalization behavior could explain the lower correlations between the model's density pre-

dictions and acoustic detections and highlights the importance of accounting for demographic and geographic variability in vocal behavior when evaluating acoustic detections, especially when treating acoustic detection rate as a proxy for density. We advise continued research into vocal behavior throughout the right whale's range, particularly in the MAB where data are especially lacking. We recommend that future PAM deployments utilize sensors and array configurations capable of estimating distances (and,

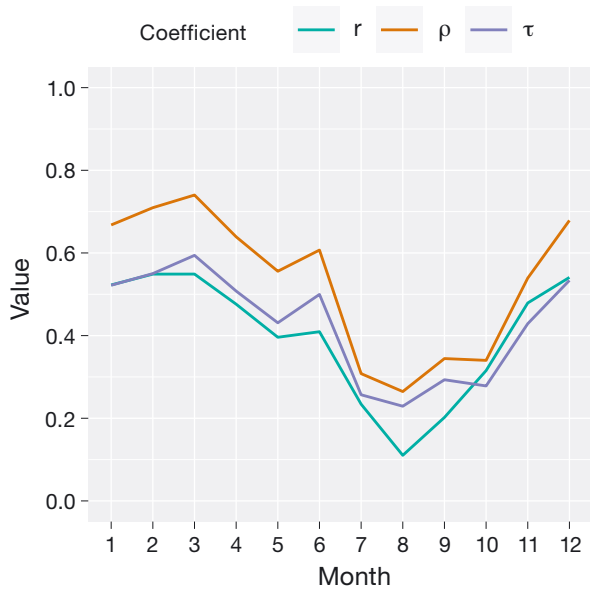


Fig. 9. Pearson's r , Spearman's ρ , and Kendall's τ correlation coefficients as calculated in Fig. 8, by month, for density predictions and acoustic data in the 2010–2019 era (October 2010–September 2020). The number of records per month ranged from 146 to 203

ideally, bearings) to vocalizing whales, especially in areas and time periods that are difficult to survey visually, so that PAM data can be directly incorporated into density models, or visual and PAM data can otherwise be modeled jointly. Until that time, species managers should be sure to consider models and results developed from both modes of monitoring when making management decisions.

Seasonally, a significant drop in correlation occurred during July–October (Fig. 9), when many right whales were believed to be in Canadian waters and US visual survey programs reduced effort. The areas of most significant mismatch were north of Cape Cod and south–southwest of Nantucket, both places where whales were acoustically detected every month of the year, but visual survey effort was relatively low during July–October and very low density was predicted. This discrepancy highlights the importance of both monitoring modes. We recommend increased visual surveying in summer and fall at these 2 locations, and in fall throughout all of US waters, to better characterize density in these locations and seasons.

For this analysis, we developed a practical method for evaluating cetacean density surface model predictions with acoustic presence rates obtained from passive acoustic monitoring. This method is readily applicable to other species and regions where similar

data exist. For example, while building this right whale density model, we also modeled 29 other cetacean taxa using the same methodology (Roberts et al. 2023). This included models for blue, fin, humpback, and sei whales, for which acoustic presence data similar to that we used for right whales are readily available (Davis et al. 2020). The same evaluation exercise could be performed for those species.

4.3. Model improvements

The only aerial program that estimated perception bias corrections was NOAA AMAPPS, and we applied the AMAPPS corrections to all programs. AMAPPS flew bubble-window aircraft at 600 ft (~183 m) altitude, but most other programs flew flat-window aircraft at 1000 ft (~305 m) and may have missed more whales along the transect line, requiring a stronger perception bias correction. By applying AMAPPS' weaker correction to the other programs, we might have biased density low on their transects. We recommend all programs develop perception bias corrections, and that funding agencies provide support for these critical data. Similarly, when developing availability bias corrections for aerial surveys of the MAB and GOM, we lacked the data needed to correct for regional and seasonal differences in diving behavior, except in CCB, the GSC, and Canadian basins, where dive data exist (e.g. Cetacean and Turtle Assessment Program 1982, Baumgartner et al. 2017, Ganley et al. 2019). Estimates for most of the MAB and GOM were based on data collected during spring at the GSC. If the diving behavior changed in other locations or times of year (e.g. during migrations), then we might have undercorrected availability bias in those situations. We recommend continued study of right whale dive behavior throughout the species' range and life cycle, ideally culminating in the development of a comprehensive model of dive behavior that synthesizes all the extant knowledge and that could drive the estimation of availability bias in models such as ours.

To address regional differences in species–habitat relationships, we modeled our 3 focal regions independently. This precluded sharing information between regions during model fitting and failed to address covariance between regions directly (e.g. when fewer whales migrated to the SAB, more remained in the MAB or GOM). Although the use of temporal covariates (Year and Era) alleviated this problem somewhat, the model might be improved by taking a hierarchical approach in which a single model is fitted to all data and covariate relationships

are allowed to vary regionally via factor-smoother interactions (Pedersen et al. 2019, Mannocci et al. 2020). Better results might also be obtained from covariates more proximal to right whale feeding habitat; these could be derived from newly-developed zooplankton distribution models (Ross et al. 2023). By focusing a follow-up analysis on species–habitat relationships and leveraging covariates from ocean climate models, it may be possible to forecast future right whale density patterns under projected climate change (Ross et al. 2021). Finally, recent methodological innovations could allow future density models to incorporate additional data not utilizable under traditional density surface modeling, such as photographic identifications of right whales (Gowan et al. 2021), surveys that did not collect sighting distances, or presence-only data such as opportunistic sightings (Wikgren et al. 2014, Gelfand & Schliep 2018).

4.4. Management applications

Most management applications, such as agency rulemaking and permitting, are based on an assumed future distribution of right whales. Given that explicit forecasts of future density are not yet available, managers usually rely on the recent past as a proxy for the near future. In this vein, our mean monthly density surfaces for the 2010–2019 era (October 2010–September 2020) are appropriate for managers to consider for this purpose. For those interested, we also provide surfaces for the 2003–2009 and 2003–2019 eras but note that these are not appropriate to use as proxies for the near future. We also provide SE and CV surfaces that depict the variability that would result if a random single year within the summary period was selected instead of the multi-year mean. For users seeking to propagate uncertainty from our model into their own models via bootstrapping, we can provide on request a set of alternative density surfaces predicted by simulated alternative models (Miller et al. 2022).

We selected 2010 as the start of our summary era based on a confluence of events centered on that year but note that significant species distribution changes occurred both before and after. For example, large aggregations first appeared in CCB in 2008 (Ganley et al. 2019), daily acoustic occurrence off Gaspé in the GSL quadrupled in 2015 (Simard et al. 2019), and the SNE area experienced sustained growth in winter and spring abundance from 2013 to 2019 (O'Brien et al. 2022). As changes continue to occur and additional data accumulate, we will revisit the best era for sum-

marization in future model updates. For management purposes, it is important to note that the spatiotemporal distribution of right whales remains highly dynamic, and thus uncertainty estimates, as well as rapidly adaptable spatiotemporal management measures, should be considered when making decisions. Where resources allow deployment of continuous monitoring approaches that have been determined to detect whales effectively and that report results in near real time, managers could consider highly dynamic mitigations, e.g. that rapidly redirect or relocate harmful activities when whales are present, when such mitigations are practicable. Consideration should be given to multiple data sources, models, perspectives, sources of expertise, and possible solutions, rather than to a single model output or approach to mitigation. In the face of high uncertainty and variability in where right whales are, the most effective mitigations may be those that apply very broadly, or do not have a spatiotemporal component at all.

Acknowledgements. Above all, we thank the observers, scientists, engineers, pilots, captains, and crews who collected the cetacean and covariate observations that formed the core of this analysis; we hope you find this project a worthwhile outcome of your efforts. A special thanks to colleagues who shared valuable advice or assisted with data preparation: Sue Barco, Elizabeth Becker, Danielle Cholewiak, Ana Cañadas, Peter Corkeron, Erin W. Cummings, Megan Ferguson, Karin Forney, Beth Josephson, David L. Miller, Richard Pace, Robert Schick, Doug Sigourney, and Len Thomas. We are grateful to Matthieu Authier and 2 anonymous reviewers for thoughtful comments that improved this paper. Corrie Curtice was our project manager. We thank all of the following for providing acoustic data: Sofie M. Van Parijs, Joel Bell, Jacqueline Bort Thornton, Gary Buchanan, Russell A. Charif, Danielle Cholewiak, Christopher W. Clark, Peter Corkeron, Julien Delarue, Kathleen Dudzinski, Robert Dziak, Jason Gedamke, Leila Hatch, Samara Haver, John Hildebrand, Lynne Hodge, Holger Klinck, Bruce Martin, David K. Mellinger, Hilary Moors-Murphy, Sharon Nieuwkerk, Susan Parks, Andrew J. Read, Aaron N. Rice, Denise Risch, Howard Rosenbaum, Melissa Soldevilla, Joy E. Stanistreet, Erin Summers, Christopher Tremblay, Sean Todd, Ann Warde, and David Wiley. Acoustic analysis was performed by Julianne Wilder, Nicole Pegg, Taylor Broadhead, Margaret Daly, Molly Martin, Alyssa Scott, Sarah Weiss, and Daniel Woodrich. Funding for visual and acoustic surveys was provided by NOAA Fisheries, NOAA Ocean Acoustics Program; National Oceanic Partnership Program (NOPP); US Navy, Navy N45, US Fleet Forces Command, and Naval Facilities Engineering Systems Command Atlantic (NAVFAC); Bureau of Ocean and Energy Management; US Coast Guard; US Army Corps of Engineers; Fisheries and Oceans Canada/Oceans and Coastal Management/Species at Risk Management, and Strategic Program for Ecosystem-Based Research and Advice funds; Georgia Department of Natural Resources; Maine Department of Marine Resources; Massachusetts

Clean Energy Center; New Jersey Department of Environmental Protection and the New Jersey Clean Energy Fund; New York State Department of Environmental Conservation; Virginia Coastal Zone Management Program; Conservation Law Foundation; National Ocean Protection Coalition; Natural Resources Defense Council; and Cornell University. Funding for the development of HYCOM has been provided by NOPP and the Office of Naval Research. Data assimilative products using HYCOM are funded by the US Navy. The 1/12 degree global HYCOM+NCODA Ocean Reanalysis was funded by the US Navy and the Modeling and Simulation Coordination Office. Computer time for HYCOM was made available by the DoD High Performance Computing Modernization Program. The output is publicly available at <https://hycom.org>. This analysis was conducted using EU Copernicus Marine Service Information. CCMP vector wind analyses were produced by Remote Sensing Systems. Data are available at <https://www.remss.com>. This analysis was funded by NOAA Fisheries (Cooperative Agreement NA20NMF0080246) and the US Navy (Cooperative Agreement N62470-20-2-2011). The results and conclusions, as well as any views or opinions expressed herein, are those of the authors and do not necessarily reflect the views of NMFS, NOAA, or the Department of Commerce.

LITERATURE CITED

- Atlas R, Hoffman RN, Ardizzone J, Leidner SM, Jusem JC, Smith DK, Gombos D (2011) A cross-calibrated, multiplatform ocean surface wind velocity product for meteorological and oceanographic applications. *Bull Am Meteorol Soc* 92:157–174
- Barlow J, Forney KA (2007) Abundance and population density of cetaceans in the California Current ecosystem. *Fish Bull* 105:509–526
- Baumgartner MF, Wenzel FW, Lysiak NSJ, Patrician MR (2017) North Atlantic right whale foraging ecology and its role in human-caused mortality. *Mar Ecol Prog Ser* 581:165–181
- Becker JJ, Sandwell DT, Smith WHF, Braud J and others (2009) Global bathymetry and elevation data at 30 arc seconds resolution: SRTM30_PLUS. *Mar Geod* 32:355–371
- Becker EA, Forney KA, Miller DL, Barlow J, Rojas-Bracho L, Urbán RJ, Moore JE (2022) Dynamic habitat models reflect interannual movement of cetaceans within the California Current ecosystem. *Front Mar Sci* 9:829523
- Behrenfeld MJ, Falkowski PG (1997) Photosynthetic rates derived from satellite-based chlorophyll concentration. *Limnol Oceanogr* 42:1–20
- Behrenfeld MJ, Boss E, Siegel DA, Shea DM (2005) Carbon-based ocean productivity and phytoplankton physiology from space. *Global Biogeochem Cycles* 19:GB10006
- Bouchet PJ, Miller DL, Roberts JJ, Mannocci L, Harris CM, Thomas L (2020) Dsmextra: extrapolation assessment tools for density surface models. *Methods Ecol Evol* 11:1464–1469
- Brasnett B (2008) The impact of satellite retrievals in a global sea-surface-temperature analysis. *Q J R Meteorol Soc* 134:1745–1760
- Brilliant SW, Vanderlaan ASM, Rangeley RW, Taggart CT (2015) Quantitative estimates of the movement and distribution of North Atlantic right whales along the northeast coast of North America. *Endang Species Res* 27:141–154
- Buckland ST, Anderson DR, Burnham KP, Laake JL, Borchers DL, Thomas L (2001) Introduction to distance sampling: estimating abundance of biological populations. Oxford University Press, Oxford
- Burt ML, Borchers DL, Jenkins KJ, Marques TA (2014) Using mark–recapture distance sampling methods on line transect surveys. *Methods Ecol Evol* 5:1180–1191
- Canny J (1986) A computational approach to edge detection. *IEEE Trans Pattern Anal Mach Intell PAMI* 8:679–698
- Carretta JV, Lowry MS, Stinchcomb CE, Lynn MS, Cosgrove RE (2000) Distribution and abundance of marine mammals at San Clemente Island and surrounding offshore waters: results from aerial and ground surveys in 1998 and 1999. NOAA Administrative Report LJ-00-02. NOAA National Marine Fisheries Service, Southwest Fisheries Center, La Jolla, CA
- Cetacean and Turtle Assessment Program (1982) CETAP: a characterization of marine mammals and turtles in the Mid- and North Atlantic areas of the U.S. outer continental shelf: final report. University of Rhode Island Graduate School of Oceanography, Kingston, RI
- Chassignet EP, Hurlburt HE, Metzger EJ, Smedstad OM and others (2009) US GODAE: Global ocean prediction with the HYbrid Coordinate Ocean Model (HYCOM). *Oceanography* 22:64–75
- Chavez-Rosales S, Palka DL, Garrison LP, Josephson EA (2019) Environmental predictors of habitat suitability and occurrence of cetaceans in the western North Atlantic Ocean. *Sci Rep* 9:5833
- Cleveland WS, Devlin SJ (1988) Locally weighted regression: an approach to regression analysis by local fitting. *J Am Stat Assoc* 83:596–610
- Cole T, Gerrior P, Merrick RL (2007) Methodologies of the NOAA National Marine Fisheries Service Aerial Survey Program for Right Whales (*Eubalaena glacialis*) in the Northeast U.S., 1998–2006. Northeast Fisheries Science Center Reference Document 07-02. NOAA National Marine Fisheries Service, Northeast Fisheries Science Center, Woods Hole, MA
- Cole TVN, Hamilton P, Henry AG, Duley P, Pace RM III, White BN, Frasier T (2013) Evidence of a North Atlantic right whale *Eubalaena glacialis* mating ground. *Endang Species Res* 21:55–64
- Crema S, Llana M, Calsamiglia A, Estrany J, Marchi L, Vericat D, Cavalli M (2020) Can inpainting improve digital terrain analysis? Comparing techniques for void filling, surface reconstruction and geomorphometric analyses. *Earth Surf Process Landf* 45:736–755
- Crowe LM, Brown MW, Corkeron PJ, Hamilton PK and others (2021) In plane sight: a mark–recapture analysis of North Atlantic right whales in the Gulf of St. Lawrence. *Endang Species Res* 46:227–251
- Crum N, Gowan T, Krzystan A, Martin J (2019) Quantifying risk of whale–vessel collisions across space, time, and management policies. *Ecosphere* 10:e02713
- Davies KTA, Brilliant SW (2019) Mass human-caused mortality spurs federal action to protect endangered North Atlantic right whales in Canada. *Mar Policy* 104:157–162
- Davies KTA, Vanderlaan ASM, Smedbol RK, Taggart CT (2015) Oceanographic connectivity between right whale critical habitats in Canada and its influence on whale abundance indices during 1987–2009. *J Mar Syst* 150:80–90
- Davies KTA, Brown MW, Hamilton PK, Knowlton AR, Taggart CT, Vanderlaan ASM (2019) Variation in North Atlantic right whale *Eubalaena glacialis* occurrence in

- the Bay of Fundy, Canada, over three decades. *Endang Species Res* 39:159–171
- ✦ Davis GE, Baumgartner MF, Bonnell JM, Bell J and others (2017) Long-term passive acoustic recordings track the changing distribution of North Atlantic right whales (*Eubalaena glacialis*) from 2004 to 2014. *Sci Rep* 7:13460
- ✦ Davis GE, Baumgartner MF, Corkeron PJ, Bell J and others (2020) Exploring movement patterns and changing distributions of baleen whales in the western North Atlantic using a decade of passive acoustic data. *Glob Change Biol* 26:4812–4840
- ✦ Delarue JJY, Moors-Murphy H, Kowarski KA, Davis GE, Urazghildiiev IR, Martin SB (2022) Acoustic occurrence of baleen whales, particularly blue, fin, and humpback whales, off eastern Canada, 2015–2017. *Endang Species Res* 47:265–289
- D'Errico J (2006) *Inpaint_nans*: MATLAB Central File Exchange. https://www.mathworks.com/matlabcentral/fileexchange/4551-inpaint_nans
- ✦ Derville S, Buell TV, Corbett KC, Hayslip C, Torres LG (2023) Exposure of whales to entanglement risk in Dungeness crab fishing gear in Oregon, USA, reveals distinctive spatio-temporal and climatic patterns. *Biol Conserv* 281:109989
- ✦ Dixon WJ (1960) Simplified estimation from censored normal samples. *Ann Math Stat* 31:385–391
- ✦ Engelhaupt DT, Pusser T, Aschettino JM, Engelhaupt AG, Cotter MP, Richlen MF, Bell JT (2020) Blue whale (*Balaenoptera musculus*) sightings off the coast of Virginia. *Mar Biodivers Rec* 13:6
- Eppley RW (1972) Temperature and phytoplankton growth in the sea. *Fish Bull* 70:1063–1085
- ✦ Franklin KJ, Cole TVN, Cholewiak DM, Duley PA and others (2022) Using sonobuoys and visual surveys to characterize North Atlantic right whale (*Eubalaena glacialis*) calling behavior in the Gulf of St. Lawrence. *Endang Species Res* 49:159–174
- ✦ Ganley LC, Brault S, Mayo CA (2019) What we see is not what there is: estimating North Atlantic right whale *Eubalaena glacialis* local abundance. *Endang Species Res* 38:101–113
- ✦ Garnesson P, Mangin A, Fanton d'Andon O, Demaria J, Bretagnon M (2019) The CMEMS GlobColour chlorophyll a product based on satellite observation: multi-sensor merging and flagging strategies. *Ocean Sci* 15:819–830
- Garrison LP, Adams J, Patterson EM, Good CP (2022) Assessing the risk of vessel strike mortality in North Atlantic right whales along the U.S. East Coast. NOAA Tech Memo NMFS-SEFSC-757. NOAA National Marine Fisheries Service, Southeast Fisheries Science Center, Miami, FL
- Gelfand AE, Schliep EM (2018) Bayesian inference and computing for spatial point patterns. Institute of Mathematical Statistics, Beachwood, OH; and American Statistical Association, Alexandria, VA
- Gillespie D (2004) Detection and classification of right whale calls using an 'edge' detector operating on a smoothed spectrogram. *Can Acoust* 32:39–47
- Good CP (2008) Spatial ecology of the North Atlantic right whale (*Eubalaena glacialis*). PhD dissertation, Duke University, Durham, NC
- ✦ Gowan TA, Ortega-Ortiz JG (2014) Wintering habitat model for the North Atlantic right whale (*Eubalaena glacialis*) in the southeastern United States. *PLOS ONE* 9:e95126
- ✦ Gowan TA, Ortega-Ortiz JG, Hostetler JA, Hamilton PK and others (2019) Temporal and demographic variation in partial migration of the North Atlantic right whale. *Sci Rep* 9:353
- ✦ Gowan TA, Crum NJ, Roberts JJ (2021) An open spatial capture–recapture model for estimating density, movement, and population dynamics from line-transect surveys. *Ecol Evol* 11:7354–7365
- ✦ Hammond PS, Macleod K, Berggren P, Borchers DL and others (2013) Cetacean abundance and distribution in European Atlantic shelf waters to inform conservation and management. *Biol Conserv* 164:107–122
- ✦ Hammond PS, Francis TB, Heinemann D, Long KJ and others (2021) Estimating the abundance of marine mammal populations. *Front Mar Sci* 8:735770
- ✦ Hansen RG, Boye TK, Larsen RS, Nielsen NH and others (2018) Abundance of whales in West and East Greenland in summer 2015. *NAMMCO Sci Publ* 11. <https://doi.org/10.7557/3.4689>
- ✦ Hedley SL, Buckland ST (2004) Spatial models for line transect sampling. *J Agric Biol Environ Stat* 9:181–199
- ✦ Heide-Jørgensen MP, Laidre KL, Hansen RG, Burt ML and others (2012) Rate of increase and current abundance of humpback whales in West Greenland. *J Cetacean Res Manag* 12:1–14
- ✦ Keller CA, Garrison L, Baumstark R, Ward-Geiger LI, Hines E (2012) Application of a habitat model to define calving habitat of the North Atlantic right whale in the southeastern United States. *Endang Species Res* 18:73–87
- ✦ Kenney RD (2018) What if there were no fishing? North Atlantic right whale population trajectories without entanglement mortality. *Endang Species Res* 37:233–237
- ✦ Kenney RD, Winn HE, Macaulay MC (1995) Cetaceans in the Great South Channel, 1979–1989: right whale (*Eubalaena glacialis*). *Cont Shelf Res* 15:385–414
- Kenney RD, Mayo CA, Winn HE (2001) Migration and foraging strategies at varying spatial scales in western North Atlantic right whales: a review of hypotheses. *J Cetacean Res Manag (Spec Issue)* 2:251–260
- ✦ Knowlton AR, Clark JS, Hamilton PK, Kraus SD, Pettis HM, Rolland RM, Schick RS (2022) Fishing gear entanglement threatens recovery of critically endangered North Atlantic right whales. *Conserv Sci Pract* 4:e12736
- ✦ Laake JL, Calambokidis J, Osmeck SD, Rugh DJ (1997) Probability of detecting harbor porpoise from aerial surveys: estimating $g(0)$. *J Wildl Manag* 61:63–75
- Laake J, Borchers D, Thomas L, Miller D, Bishop J (2021) *Mrds*: mark–recapture distance sampling. R package version 2.2.5. <https://CRAN.R-project.org/package=mrds>
- ✦ Leiter SM, Stone KM, Thompson JL, Accardo CM and others (2017) North Atlantic right whale *Eubalaena glacialis* occurrence in offshore wind energy areas near Massachusetts and Rhode Island, USA. *Endang Species Res* 34:45–59
- ✦ Mannocci L, Roberts JJ, Pedersen EJ, Halpin PN (2020) Geographical differences in habitat relationships of cetaceans across an ocean basin. *Ecography* 43:1250–1259
- ✦ Marques FFC, Buckland ST (2003) Incorporating covariates into standard line transect analyses. *Biometrics* 59:924–935
- ✦ Marques TA, Thomas L, Martin SW, Mellinger DK and others (2013) Estimating animal population density using passive acoustics. *Biol Rev Camb Philos Soc* 88:287–309
- ✦ Marra G, Wood SN (2011) Practical variable selection for generalized additive models. *Comput Stat Data Anal* 55:2372–2387

- Marsh H, Sinclair DF (1989) Correcting for visibility bias in strip transect aerial surveys of aquatic fauna. *J Wildl Manag* 53:1017–1024
- Martin J, Sabatier Q, Gowan TA, Giraud C and others (2016) A quantitative framework for investigating risk of deadly collisions between marine wildlife and boats. *Methods Ecol Evol* 7:42–50
- Mate BR, Nieuwkerk SL, Kraus SD (1997) Satellite-monitored movements of the northern right whale. *J Wildl Manag* 61:1393–1405
- Mayo CA, Ganley L, Hudak CA, Brault S, Marx MK, Burke E, Brown MW (2018) Distribution, demography, and behavior of North Atlantic right whales (*Eubalaena glacialis*) in Cape Cod Bay, Massachusetts, 1998–2013. *Mar Mamm Sci* 34:979–996
- Meissner T, Wentz FJ, Scott J, Vazquez-Cuervo J (2016) Sensitivity of ocean surface salinity measurements from spaceborne L-band radiometers to ancillary sea surface temperature. *IEEE Trans Geosci Remote Sens* 54:7105–7111
- Mellinger DK (2004) A comparison of methods for detecting right whale calls. *Can Acoust* 32:55–65
- Mesgaran MB, Cousens RD, Webber BL (2014) Here be dragons: a tool for quantifying novelty due to covariate range and correlation change when projecting species distribution models. *Divers Distrib* 20:1147–1159
- Meyer-Gutbrod E, Greene C, Davies K, Johns D (2021) Ocean regime shift is driving collapse of the North Atlantic right whale population. *Oceanography* 34:22–31
- Meyer-Gutbrod EL, Davies KTA, Johnson CL, Plourde S and others (2023) Redefining North Atlantic right whale habitat-use patterns under climate change. *Limnol Oceanogr* 68:S71–S86
- Miller DL, Burt ML, Rexstad EA, Thomas L (2013) Spatial models for distance sampling data: recent developments and future directions. *Methods Ecol Evol* 4:1001–1010
- Miller DL, Becker EA, Forney KA, Roberts JJ, Cañadas A, Schick RS (2022) Estimating uncertainty in density surface models. *PeerJ* 10:e13950
- Monsarrat S, Pennino MG, Smith TD, Reeves RR, Meynard CN, Kaplan DM, Rodrigues ASL (2015) Historical summer distribution of the endangered North Atlantic right whale (*Eubalaena glacialis*): a hypothesis based on environmental preferences of a congeneric species. *Divers Distrib* 21:925–937
- Monsarrat S, Pennino MG, Smith TD, Reeves RR, Meynard CN, Kaplan DM, Rodrigues ASL (2016) A spatially explicit estimate of the prewhaling abundance of the endangered North Atlantic right whale. *Conserv Biol* 30:783–791
- Moore MJ, Rowles TK, Fauquier DA, Baker JD and others (2021) Assessing North Atlantic right whale health: threats, and development of tools critical for conservation of the species. *Dis Aquat Org* 143:205–226
- Morel A (1991) Light and marine photosynthesis: a spectral model with geochemical and climatological implications. *Prog Oceanogr* 26:263–306
- Moses E, Finn JT (1997) Using Geographic Information Systems to predict North Atlantic right whale (*Eubalaena glacialis*) habitat. *J Northwest Atl Fish Sci* 22:37–46
- O'Brien O, Pendleton DE, Ganley LC, McKenna KR and others (2022) Repatriation of a historical North Atlantic right whale habitat during an era of rapid climate change. *Sci Rep* 12:12407
- Pace RM III, Corkeron PJ, Kraus SD (2017) State–space mark–recapture estimates reveal a recent decline in abundance of North Atlantic right whales. *Ecol Evol* 7:8730–8741
- Palka D, Aichinger Dias L, Broughton E, Chavez-Rosales S and others (2021) Atlantic Marine Assessment Program for Protected Species: FY15–FY19. OCS Study BOEM 2021-051. US Department of the Interior, Bureau of Ocean Energy Management, Washington, DC
- Parks SE, Cusano DA, Van Parijs SM, Nowacek DP (2019) Acoustic crypsis in communication by North Atlantic right whale mother–calf pairs on the calving grounds. *Biol Lett* 15:20190485
- Pedersen EJ, Miller DL, Simpson GL, Ross N (2019) Hierarchical generalized additive models in ecology: an introduction with mgcv. *PeerJ* 7:e6876
- Pendleton DE, Sullivan PJ, Brown MW, Cole TVN and others (2012) Weekly predictions of North Atlantic right whale *Eubalaena glacialis* habitat reveal influence of prey abundance and seasonality of habitat preferences. *Endang Species Res* 18:147–161
- Pendleton DE, Tingley MW, Ganley LC, Friedland KD and others (2022) Decadal-scale phenology and seasonal climate drivers of migratory baleen whales in a rapidly warming marine ecosystem. *Glob Change Biol* 28:4989–5005
- Pettis HM, Pace RM III, Hamilton PK (2023) North Atlantic Right Whale Consortium 2022 Annual Report Card. North Atlantic Right Whale Consortium, Boston, MA
- Quintana-Rizzo E, Leiter S, Cole TVN, Hagbloom MN and others (2021) Residency, demographics, and movement patterns of North Atlantic right whales *Eubalaena glacialis* in an offshore wind energy development area in southern New England, USA. *Endang Species Res* 45:251–268
- Record NR, Runge JA, Pendleton DE, Balch WM and others (2019) Rapid climate-driven circulation changes threaten conservation of endangered North Atlantic right whales. *Oceanography* 32:162–169
- Reed J, New L, Corkeron P, Harcourt R (2022) Multi-event modeling of true reproductive states of individual female right whales provides new insights into their decline. *Front Mar Sci* 9:994481
- Roarty H, Glenn S, Brodie J, Nazzaro L and others (2020) Annual and seasonal surface circulation over the Mid-Atlantic Bight Continental Shelf derived from a decade of High Frequency Radar observations. *J Geophys Res Oceans* 125:e2020JC016368
- Roberts JJ, Best BD, Dunn DC, Trembl EA, Halpin PN (2010) Marine Geospatial Ecology Tools: an integrated framework for ecological geoprocessing with ArcGIS, Python, R, MATLAB, and C++. *Environ Model Softw* 25:1197–1207
- Roberts JJ, Best BD, Mannocci L, Fujioka E and others (2016) Habitat-based cetacean density models for the U.S. Atlantic and Gulf of Mexico. *Sci Rep* 6:22615
- Roberts JJ, Yack TM, Halpin PN (2023) Marine mammal density models for the U.S. Navy Atlantic Fleet Training and Testing (AFTT) study area for the Phase IV Navy Marine Species Density Database (NMSDD), Document Version 1.3. Duke University Marine Geospatial Ecology Laboratory, Durham, NC
- Ross CH, Pendleton DE, Tupper B, Brickman D, Zani MA, Mayo CA, Record NR (2021) Projecting regions of North Atlantic right whale, *Eubalaena glacialis*, habitat suitability in the Gulf of Maine for the year 2050. *Elementa Sci Anthropocene* 9:00058
- Ross CH, Runge JA, Roberts JJ, Brady DC, Tupper B, Record

- NR (2023) Estimating North Atlantic right whale prey based on *Calanus finmarchicus* thresholds. *Mar Ecol Prog Ser* 703:1–16
- ✦ Schick RS, Halpin PN, Read AJ, Urban DL and others (2011) Community structure in pelagic marine mammals at large spatial scales. *Mar Ecol Prog Ser* 434:165–181
- ✦ Schick RS, Kraus SD, Rolland RM, Knowlton AR and others (2013) Using hierarchical Bayes to understand movement, health, and survival in the endangered North Atlantic right whale. *PLOS ONE* 8:e64166
- ✦ Seim H, Savidge D, Andres M, Bane J and others (2022) Overview of the Processes Driving Exchange at Cape Hatteras program. *Oceanography* 35:6–17
- ✦ Sharp SM, McLellan WA, Rotstein DS, Costidis AM and others (2019) Gross and histopathologic diagnoses from North Atlantic right whale *Eubalaena glacialis* mortalities between 2003 and 2018. *Dis Aquat Org* 135:1–31
- ✦ Silsbe GM, Behrenfeld MJ, Halsey KH, Milligan AJ, Westberry TK (2016) The CAFE model: a net production model for global ocean phytoplankton. *Global Biogeochem Cycles* 30:1756–1777
- ✦ Simard Y, Roy N, Giard S, Aulanier F (2019) North Atlantic right whale shift to the Gulf of St. Lawrence in 2015, revealed by long-term passive acoustics. *Endang Species Res* 40:271–284
- ✦ Stewart JD, Durban JW, Knowlton AR, Lynn MS and others (2021) Decreasing body lengths in North Atlantic right whales. *Curr Biol* 31:3174–3179
- ✦ Stewart JD, Durban JW, Europe H, Fearnbach H and others (2022) Larger females have more calves: influence of maternal body length on fecundity in North Atlantic right whales. *Mar Ecol Prog Ser* 689:179–189
- ✦ Thomas L, Buckland ST, Rexstad EA, Laake JL and others (2010) Distance software: design and analysis of distance sampling surveys for estimating population size. *J Appl Ecol* 47:5–14
- Townsend DW (1991) Influences of oceanographic processes on the biological productivity of the Gulf of Maine. *Rev Aquat Sci* 5:211–230
- Wentz FJ, Scott J, Hofflman R, Leidner M, Atlas R, Ardizzone J (2015) Remote Sensing Systems Cross-Calibrated Multi-Platform (CCMP) 6-hourly ocean vector wind analysis product on 0.25 deg grid, Version 2.0. Remote Sensing Systems, Santa Rosa, CA
- ✦ Westberry T, Behrenfeld MJ, Siegel DA, Boss E (2008) Carbon-based primary productivity modeling with vertically resolved photoacclimation. *Global Biogeochem Cycles* 22:GB2024
- ✦ Whitt AD, Dudzinski K, Laliberté JR (2013) North Atlantic right whale distribution and seasonal occurrence in near-shore waters off New Jersey, USA, and implications for management. *Endang Species Res* 20:59–69
- ✦ Wikgren B, Kite-Powell H, Kraus S (2014) Modeling the distribution of the North Atlantic right whale *Eubalaena glacialis* off coastal Maine by areal co-kriging. *Endang Species Res* 24:21–31
- ✦ Williams R, Hedley SL, Branch TA, Bravington MV, Zerbini AN, Findlay KP (2011) Chilean blue whales as a case study to illustrate methods to estimate abundance and evaluate conservation status of rare species. *Conserv Biol* 25:526–535
- ✦ Wood SN (2011) Fast stable restricted maximum likelihood and marginal likelihood estimation of semiparametric generalized linear models. *J R Stat Soc B* 73: 3–36
- Wood S (2017) Generalized additive models: an introduction with R, 2nd edn. CRC Press, Boca Raton, FL
- ✦ Zoidis AM, Lomac-MacNair KS, Ireland DS, Rickard ME, McKown KA, Schlesinger MD (2021) Distribution and density of six large whale species in the New York Bight from monthly aerial surveys 2017 to 2020. *Cont Shelf Res* 230:104572

Appendix. Full author addresses

Jason J. Roberts^{1,*}, Tina M. Yack¹, Ei Fujioka¹, Patrick N. Halpin¹,
 Mark F. Baumgartner², Oliver Boisseau³, Samuel Chavez-Rosales⁴,
 Timothy V. N. Cole⁵, Mark P. Cotter⁶, Genevieve E. Davis⁵,
 Robert A. DiGiovanni Jr.⁷, Laura C. Ganley⁸, Lance P. Garrison⁹,
 Caroline P. Good¹⁰, Timothy A. Gowan¹¹, Katharine A. Jackson¹¹,
 Robert D. Kenney¹², Christin B. Khan⁵, Amy R. Knowlton⁸, Scott D. Kraus⁸,
 Gwen G. Lockhart¹³, Kate S. Lomac-MacNair¹⁴, Charles A. Mayo¹⁵,
 Brigid E. McKenna⁴, William A. McLellan¹⁶, Douglas P. Nowacek^{17,18},
 Orfhlaith O'Brien⁸, D. Ann Pabst¹⁶, Debra L. Palka⁵, Eric M. Patterson¹⁰,
 Daniel E. Pendleton⁴, Ester Quintana-Rizzo¹⁹, Nicholas R. Record²⁰,
 Jessica V. Redfern⁸, Meghan E. Rickard²¹, Melanie White²², Amy D. Whitt²³,
 Ann M. Zoidis¹⁴

¹Marine Geospatial Ecology Laboratory, Duke University, Durham, NC 27708, USA

²Biology Department, Woods Hole Oceanographic Institution, Woods Hole, MA 02543, USA

³Marine Conservation Research, Kelvedon CO5 9AA, UK

⁴Integrated Statistics under contract to Northeast Fisheries Science Center, NOAA Fisheries, Woods Hole, MA 02543, USA

⁵Northeast Fisheries Science Center, NOAA Fisheries, Woods Hole, MA 02543, USA

⁶HDR, Inc., Virginia Beach, VA 23445, USA

⁷Atlantic Marine Conservation Society, Hampton Bays, NY 11946, USA

⁸Anderson Cabot Center for Ocean Life, New England Aquarium, Boston, MA 02110, USA

⁹Southeast Fisheries Science Center, NOAA Fisheries, Miami, FL 33149, USA

¹⁰Office of Protected Resources, NOAA Fisheries, Silver Spring, MD 20910, USA

¹¹Fish and Wildlife Research Institute, Florida Fish and Wildlife Conservation Commission, St. Petersburg, FL 33701, USA

¹²Graduate School of Oceanography, University of Rhode Island, Narragansett, RI 02882, USA

¹³Tetra Tech, Inc., Boston, MA 02109, USA

¹⁴Tetra Tech, Inc., Oakland, CA 94612, USA

¹⁵Center for Coastal Studies, Provincetown, MA 02657, USA

¹⁶Department of Biology and Marine Biology, University of North Carolina Wilmington, Wilmington, NC 28403, USA

¹⁷Duke University Marine Laboratory, Beaufort, NC 28516, USA

¹⁸Pratt School of Engineering, Duke University, Durham, NC 27708, USA

¹⁹Emmanuel College, Boston, MA 02155, USA

²⁰Tandy Center for Ocean Forecasting, Bigelow Laboratory for Ocean Sciences, East Boothbay, ME 04544, USA

²¹New York Natural Heritage Program, College of Environmental Science and Forestry, State University of New York, Kings Park, NY 11754, USA

²²Clearwater Marine Aquarium Research Institute, Clearwater, FL 33767, USA

²³Azura Consulting LLC, Garland, TX 75043, USA

Editorial responsibility: Elliott Hazen,
 Pacific Grove, California, USA

Reviewed by: M. Authier, L. G. Torres and 1 anonymous referee

Submitted: September 23, 2023

Accepted: January 30, 2024

Proofs received from author(s): March 18, 2024